Dust in z=1-2 infrared luminous galaxies and obscured quasars

Cristian Vignali

Dipartimento di Astronomia,

Universita` degli Studi di Bologna

In collaboration with

F. Pozzi, A. Feltre, J. Fritz, C. Gruppioni, A. Comastri, R. Gilli,
M. Mignoli, G. Zamorani, M. Brusa, F. Fiore, F. La Franca,
R. Maiolino, […]

Talk outline

- The Universe at z≈1-2: accretion vs. star-formation activity
- I sample: obscured and luminous hard X-ray selected quasars at z≈1-2: reproducing the SED via smooth torus models, and deriving accretion-related parameters
- Coeval obscured accretion and strong star formation at high redshifts: hints for an “evolutionary sequence” for AGN
- II sample: ULIRGs at z≈2 and the role of AGN. SED fitting using mid-IR (*Spitzer*) and far-IR *Herschel* photometry plus *Spitzer*-IRS spectroscopy
- Summary

Accretion and star formation over cosmic time

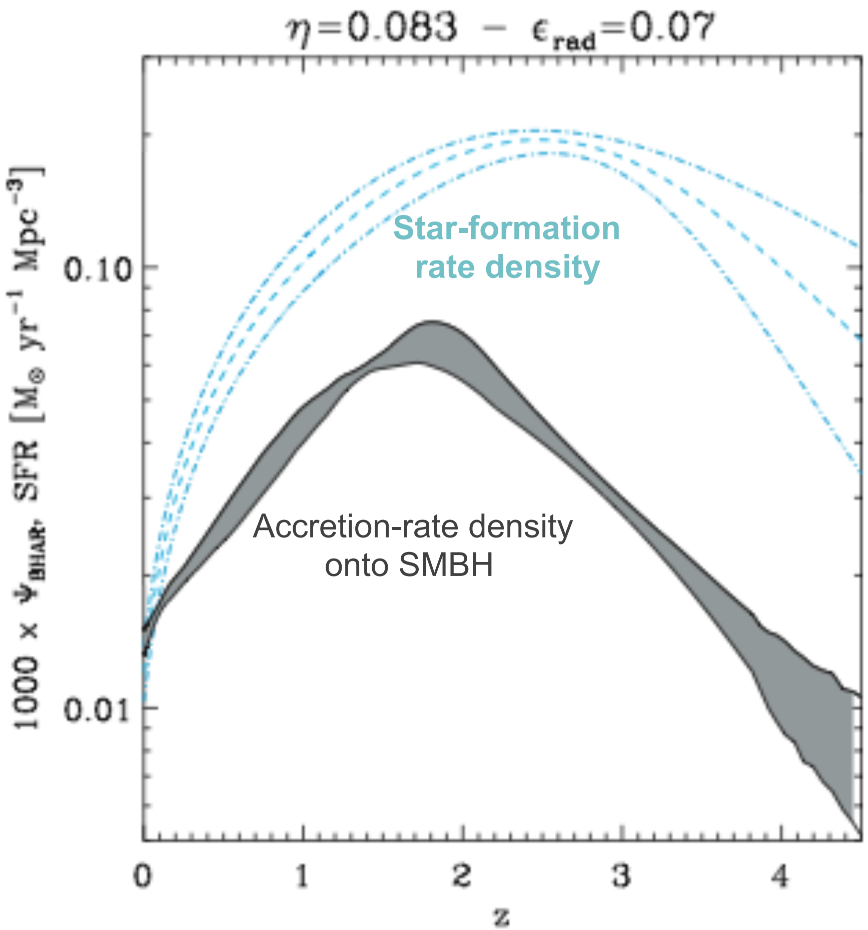

from Merloni & Heinz 2008;
see also Hopkins & Beacom 2006, Gruppioni et al. 2011

I sample: luminous obscured (Type 2) quasars at z≈1-2 selected in hard X-rays from the HELLAS2XMM survey observed with *Spitzer*

Sample selection: extreme X/O sources

SAMPLE: **HELLAS2XMM**

$F_{2\text{-}10\,keV}$ >10^{-14} erg cm^{-2} s^{-1} over 1.4 deg^2

70% spectroscopic completeness

Optically faint (R>24) sources with limited identification + "certified" (with spec-z), mostly high X-ray-to-optical flux ratio (Log(X/O)>1) sources (suggestive of X-ray obscuration)

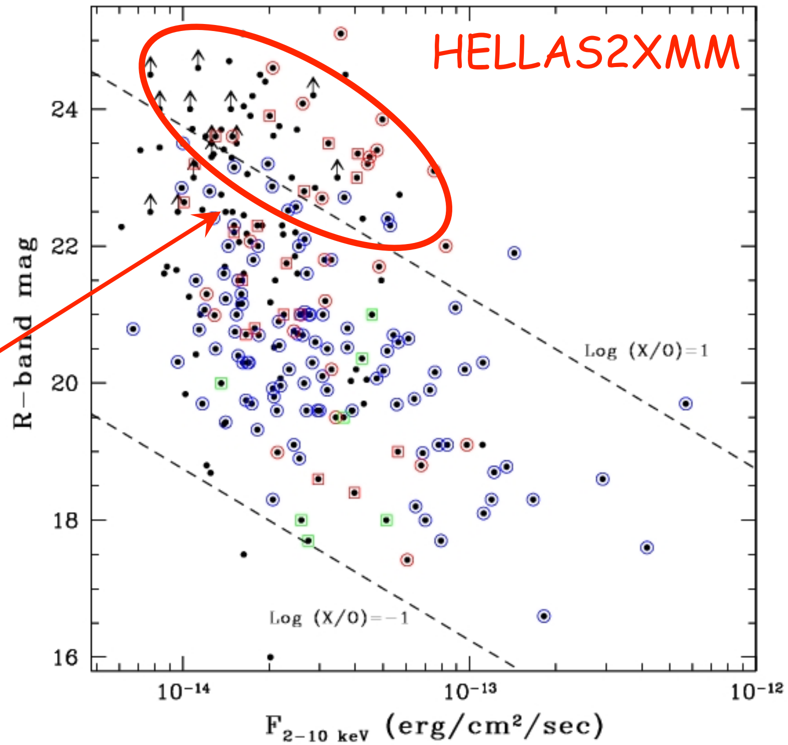

16 obscured ($<N_H>\approx 7\times10^{22}$ cm^{-2}), X-ray luminous ($L_{2\text{-}10\,keV}\approx 10^{44\text{-}45}$ erg/s) quasars at z=0.9-2.1

Spitzer data to characterize their X-ray emission and estimate bolometric luminosities

All bright in the Ks band, the most extreme being EROs (Mignoli et al. 2004)

Results presented in Pozzi et al. (2010)

Two ways to deal with IR emission from AGN: "clumpy" vs. "smooth" torus models

Method: using the reprocessed IR emission to estimate the intrinsic optical/UV luminosity ➔ NEED FOR Lbol related to accretion processes

Smooth dust distribution

dust grains around a central source (AGN) in a smooth distribution (e.g., Pier & Krolik 1992, Granato & Danese 1994; Efstathiou & Rowan-Robinson 1995, Fritz et al. 2006)

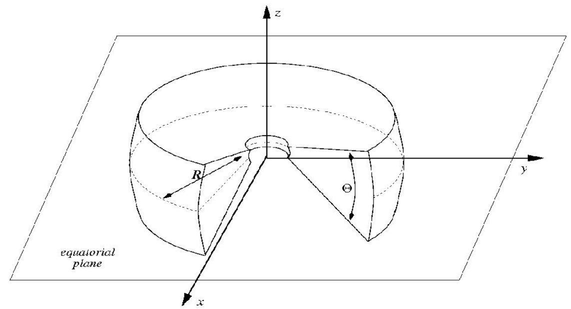

Clumpy models

dust grains in clouds (not uniform distribution). A Type 2 AGN can be seen also at large inclination angles over the equatorial plane (e.g., Nenkova et al. 2002, 2008a,b; Nikutta et al. 2009; Hoenig et al. 2008, 2010; Schartmann et al. 2008; see also Ramos-Almeida et al. 2009, 2011; Alonso-Herrero et al. 2011)

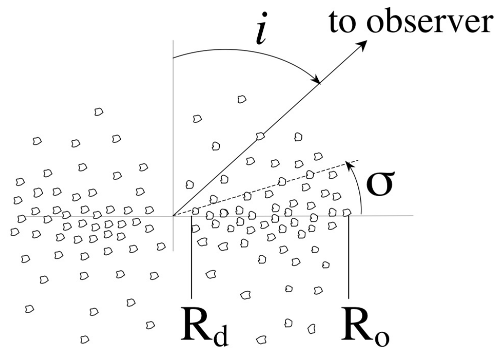

See A. Feltre's talk (Friday) for a comparison of these modelings + Nikutta's talk (yesterday) for clumpy solutions

Comparison:

- ✓ Photometric data points generally reproduced by both models (see Dullemond & Van Bemmel 05).
- ✓ 'Smooth model': simpler, well reproduces the emission feature in emission
- ✓ 'Clumpy model' in agreement with X-ray variability (i.e. Risaliti et al. 07, 10)

Indications from X-ray observations of Seyferts

Eclipses of the X-ray source are COMMON in nearby AGN: $\Delta N_H \sim 10^{23}$-10^{24} cm^{-2}

↓

size X-ray src $<10^{14}$ cm
D $< 10^{16}$ cm

↓

X-ray absorber “made” of BLR clouds

Risaliti et al., 2007, 2010…

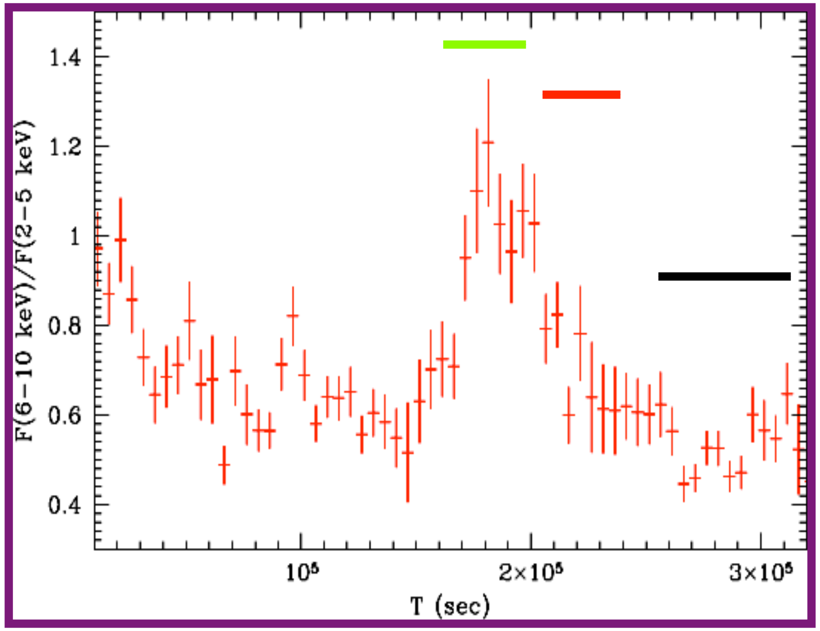

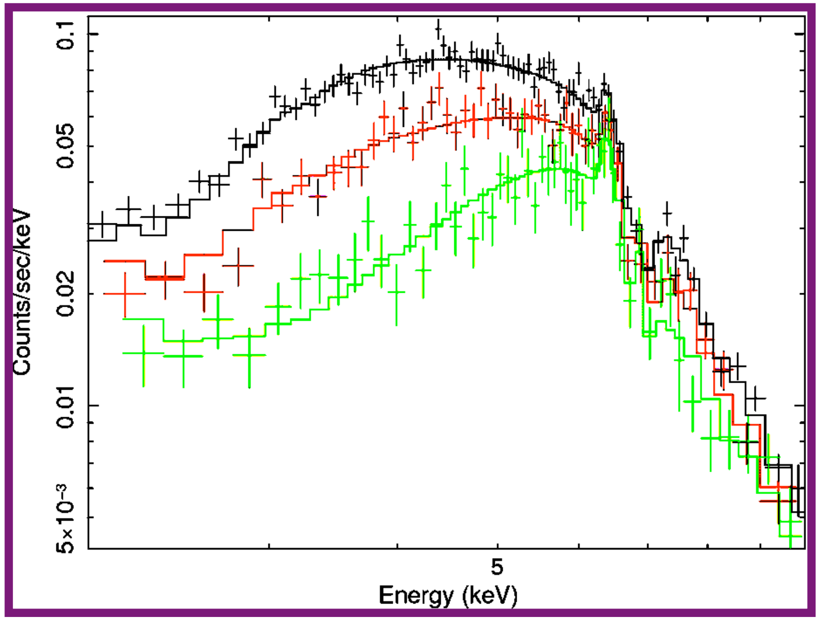

Indications from high-resolution mid-IR observations of Seyferts

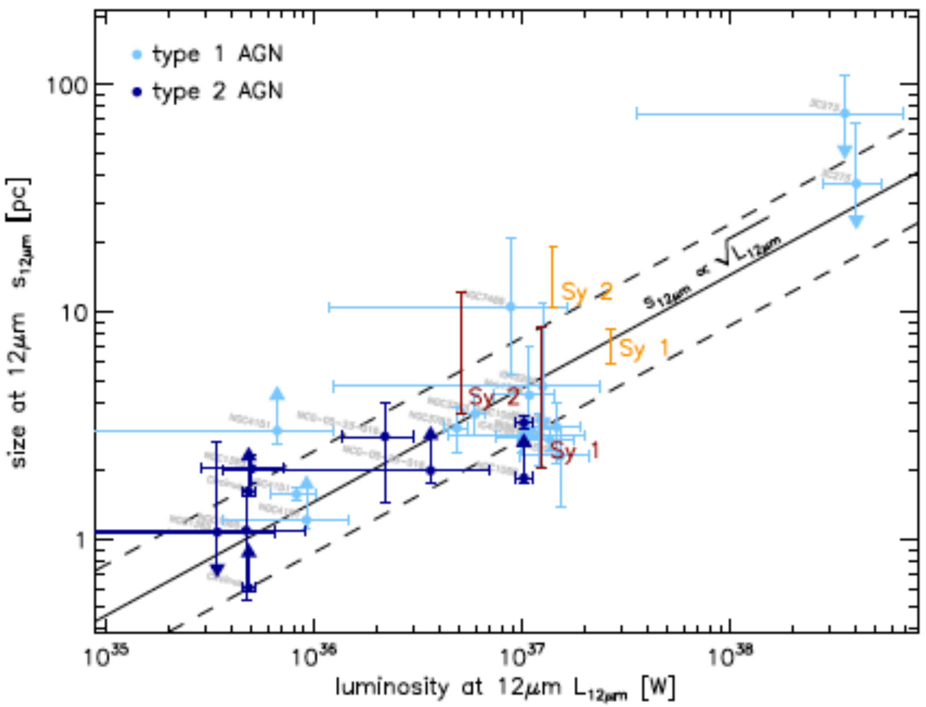

Tristram & Schartmann 2011
(see also Jaffe+04; Meisenheimer+07; Tristram+07; Tristram+09)

- Compact (a few pc) tori with a clumpy/filamentary dust distribution (warm disk + geom. thick torus)

- No significant Sey1/Sey2 difference

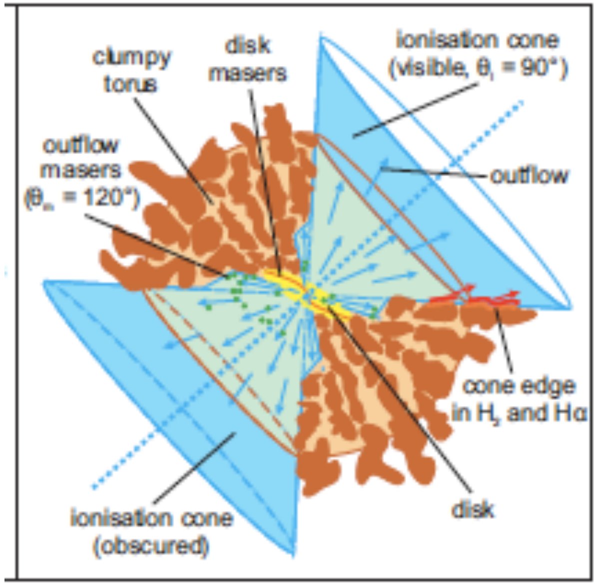

Tristram+07 - Circinus

Modeling the mid-IR emission with “clumpy” torus

✓ Type 1 vs. Type 2 AGN difference: it is a function of the number of clouds along the line of sight, i.e., of the escape probability
✓ Same dust temperatures can be observed at different distances from the AGN

➔ Type 2 AGN: larger number of clouds and lower P_{esc} for the photons to escape

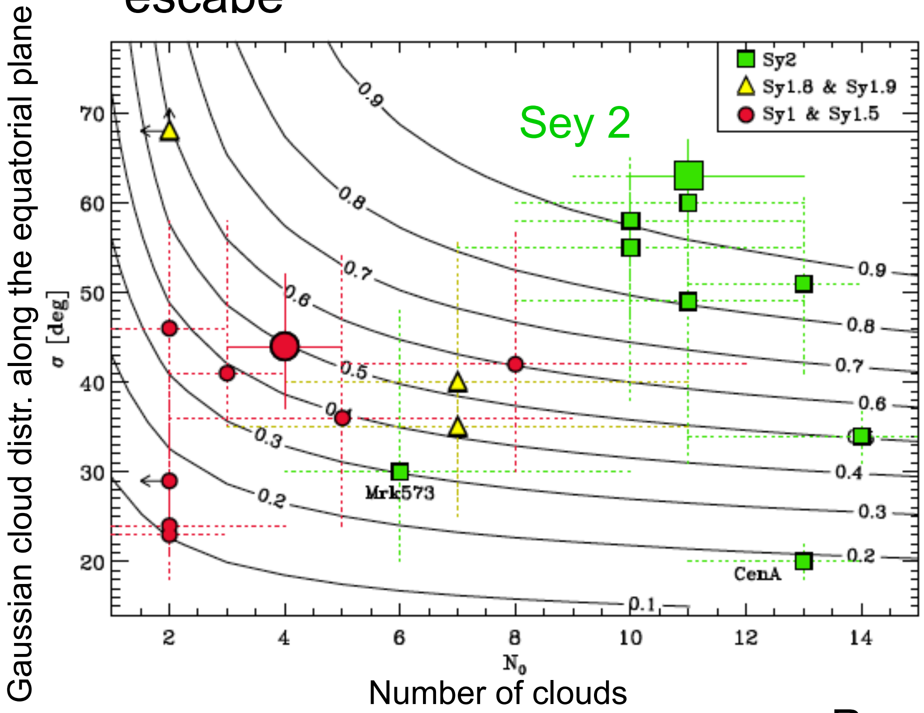

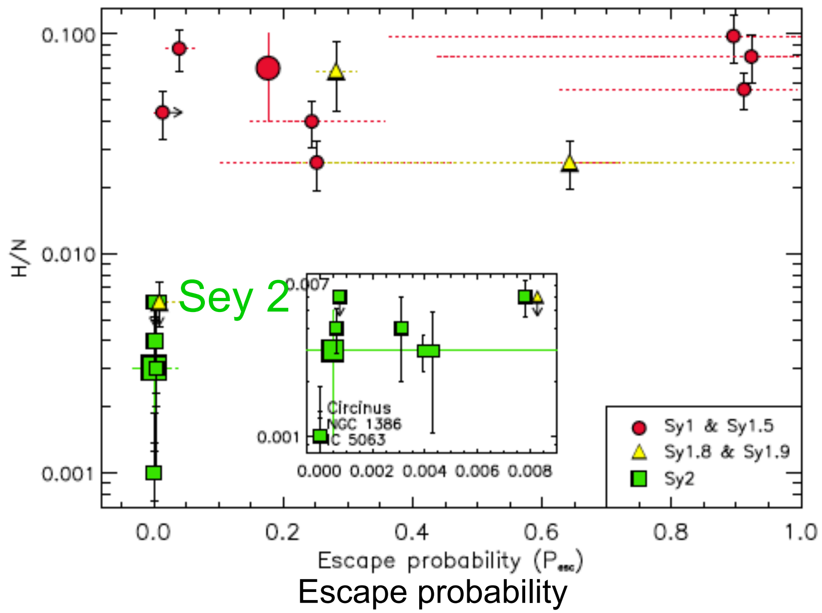

Ramos-Almeida+11

Smooth torus model: flared disk (Fritz+06)

- IR emission computed by solving the radiative transfer equations (absorption, scattering and re-emission from graphite and silicate dust grains)
- Model: original parameters:
- α, β → density distribution
- Θ → covering factor
- $\tau(9.7\mu m)$ → optical depth along the l.o.s.
- $R = R_{max}/ R_{min}$ of the torus
- ψ → line of sight (w.r.t. the eq. plane)

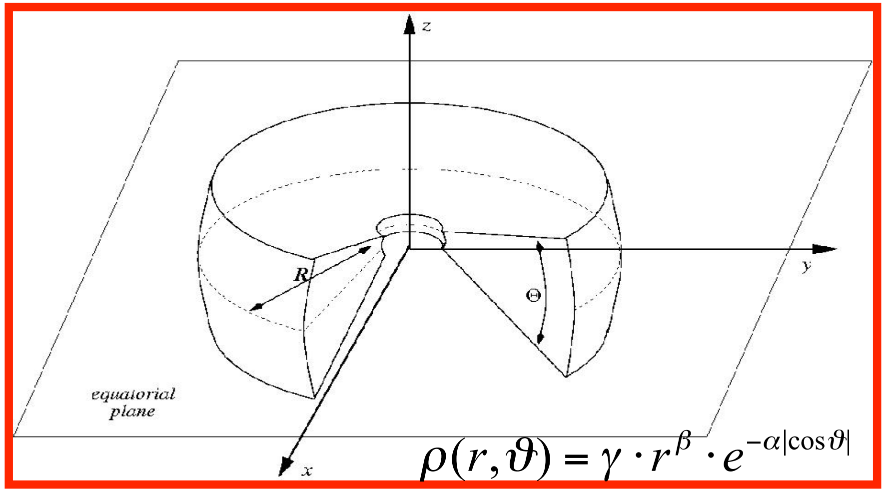

$$\rho(r,\vartheta) = \gamma \cdot r^{\beta} \cdot e^{-\alpha|\cos\vartheta|}$$

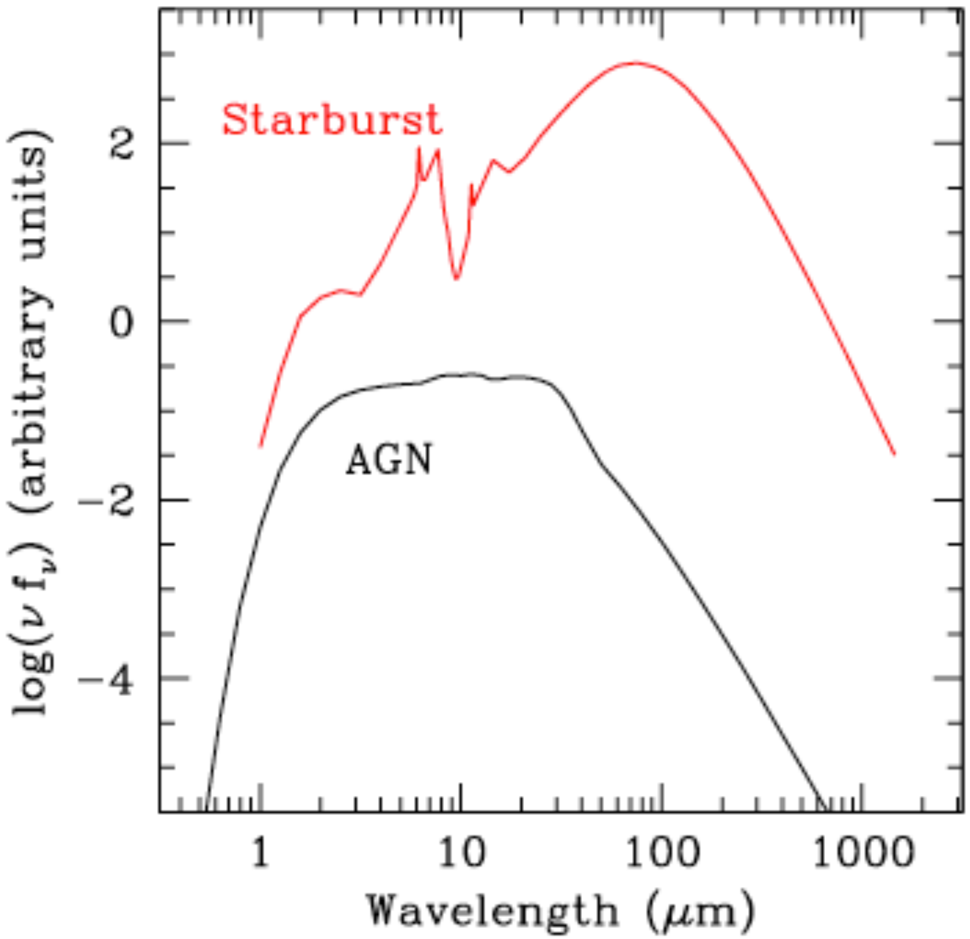

BROAD-BAND SED fitting: common problem to all torus models:
Need to separate the galaxy contribution from that due to the AGN

AGN reprocessed emission and starburst SED peak at different wavelengths

➔ need to decouple the activity due to accretion from that related to stellar processes

Smooth torus model: flared disk (Fritz+06)

- IR emission computed by solving the radiative transfer equations (absorption, scattering and re-emission from graphite and silicate dust grains)
- Model: original parameters:
- α, β $\rightarrow$ density distribution
- Θ $\rightarrow$ covering factor
- $\tau(9.7\mu m)$ $\rightarrow$ optical depth along the l.o.s.
- $R = R_{max}/ R_{min}$ of the torus
- ψ $\rightarrow$ line of sight (w.r.t. the eq. plane)

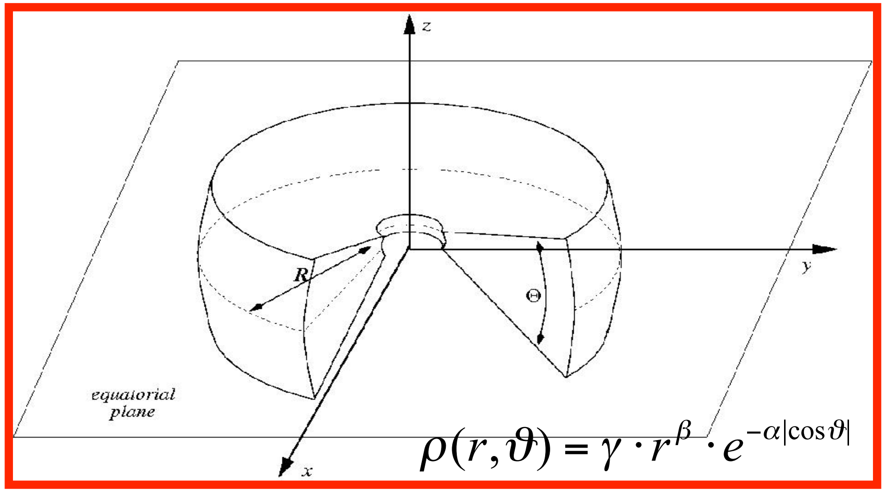

$$\rho(r,\vartheta) = \gamma \cdot r^{\beta} \cdot e^{-\alpha|\cos\vartheta|}$$

SED modeling: stars, AGN, and starburst (if data>24 μm)

- SSP for stellar population, Schmidt-like law of star formation, Chabrier IMF, MW extinction law
- AGN emission re-processed by the torus in the mid-IR (grid of >1000 models)
- starburst templates to account for the FAR-IR/sub-mm data points

Fit over the observed optical, IR (and sub-mm in one case) photometric points

Fitting model and parameter space

Limited number of photometric data points and degeneracy in the parameters

- β, Θ and $\tau(9.7\mu m)$ as free parameters
- best-fitting SED + 1σ solutions (χ^2)

Detailed discussion in A. Feltre's talk

Low $\tau_{eq}(9.7\mu m) \Rightarrow$ Silicate feature in emission

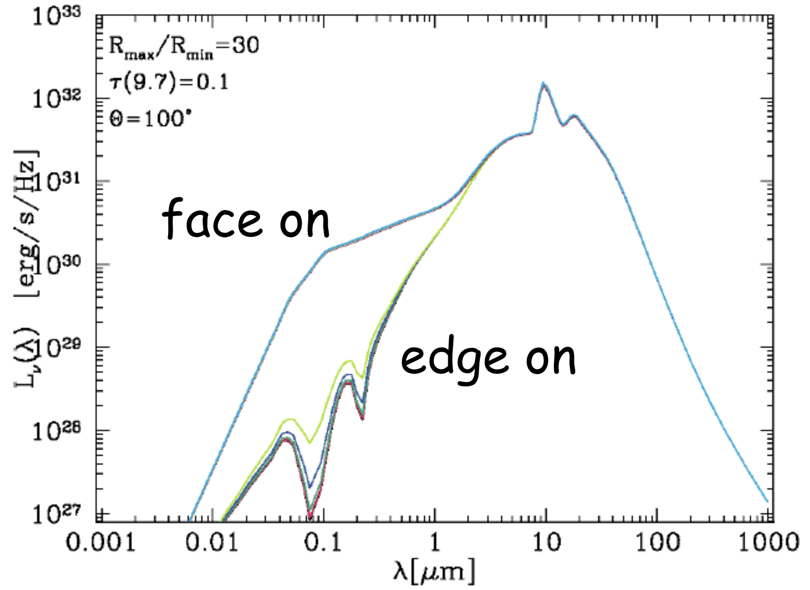

High $\tau_{eq}(9.7\mu m) \Rightarrow$ Silicate feature in absorption

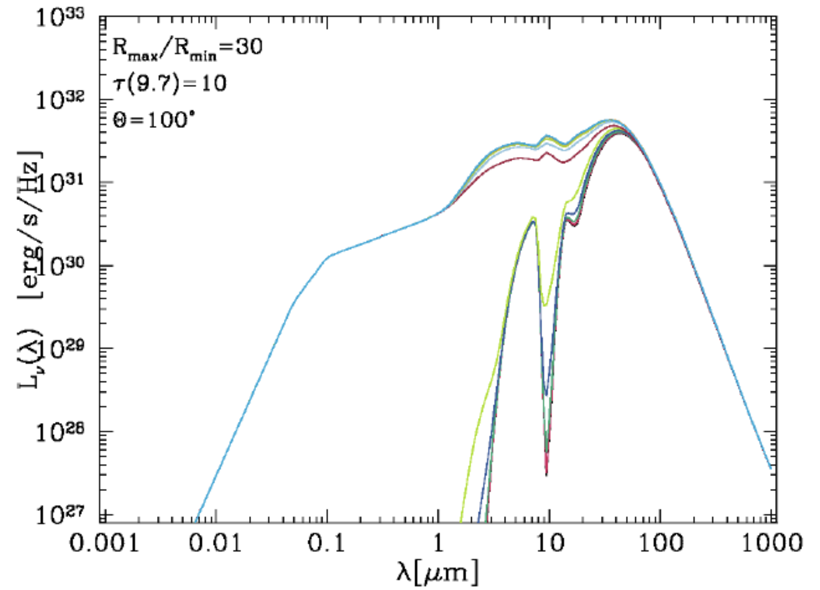

The AGN components

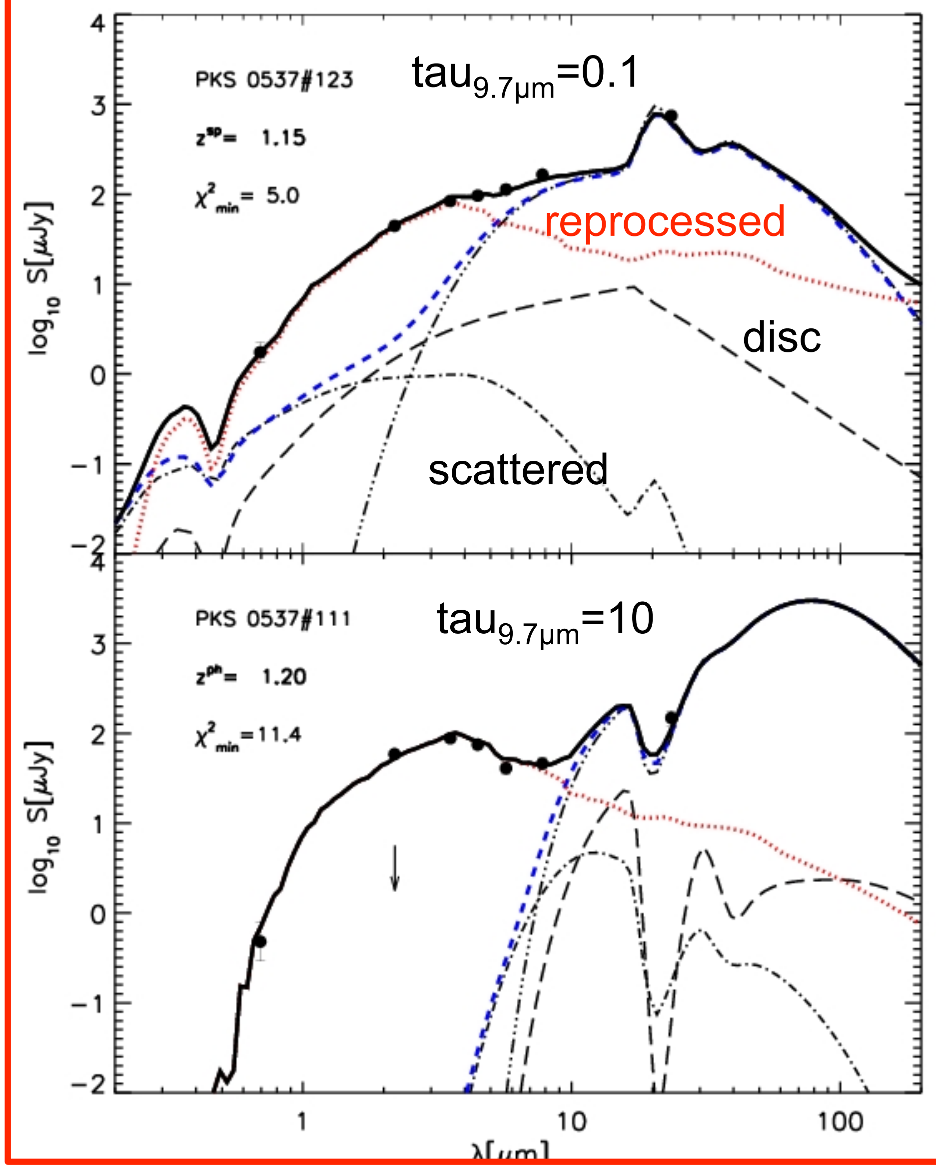

AGN components

- Torus component (reprocessed by dust)
- Disc component
- Scattered component

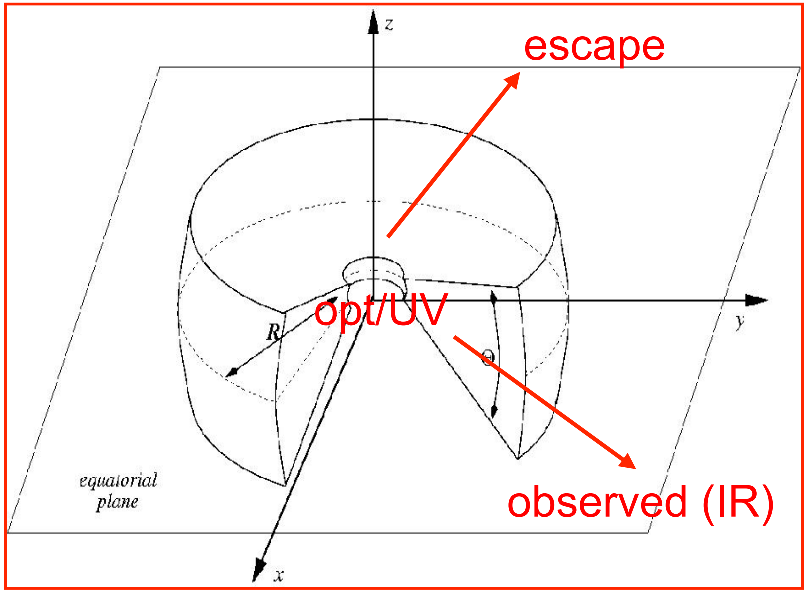

Results – I. SED “deconvolution” analysis

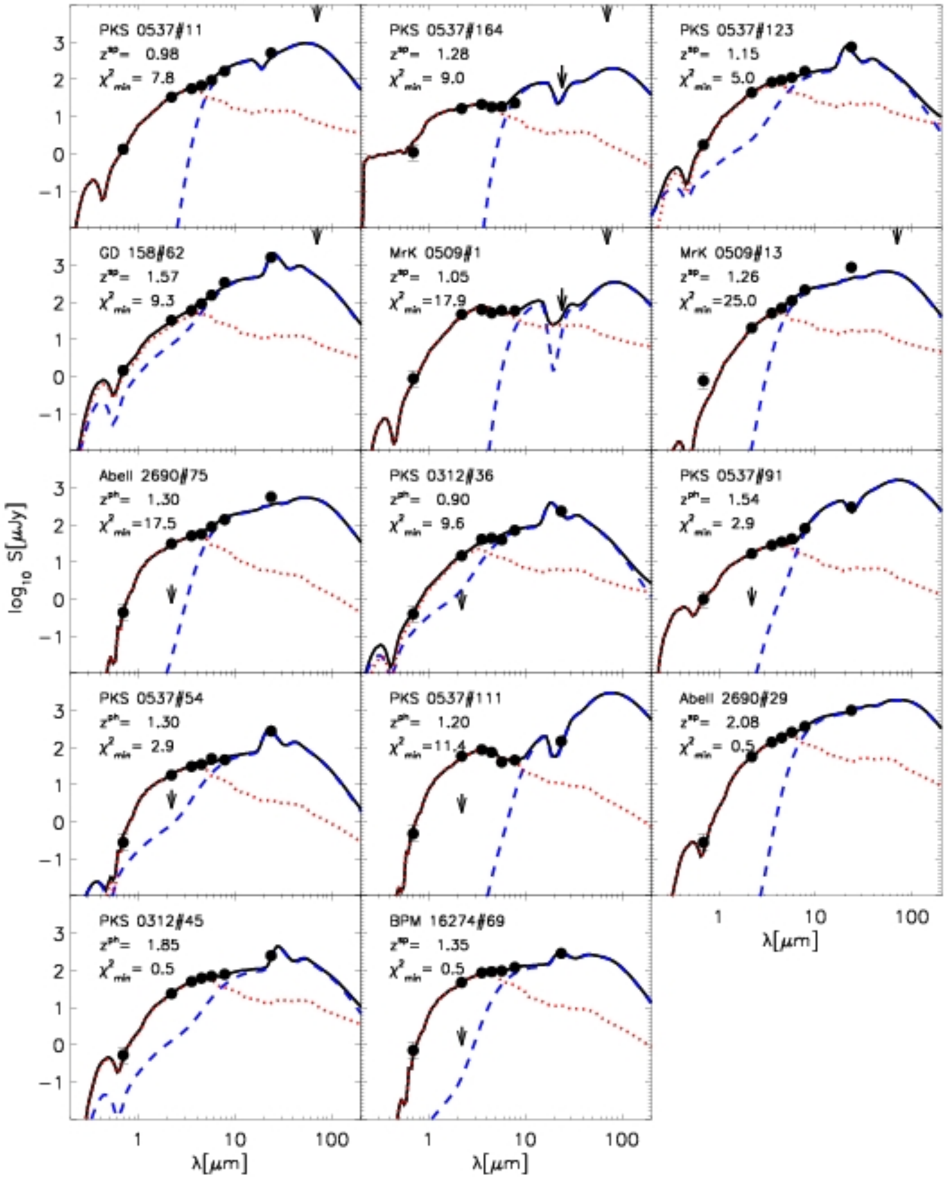

Pozzi et al., A&A (2010)

Torus (AGN)

Host Galaxy

✓ Typically, good fits to the R, K_S and *Spitzer* data

✓ Host galaxy required, prominent for extreme X/O sources

✓ Nucleus starts dominating at the longest-λ IRAC bands

✓ 80% of sources have τ(9.7μm)<3

Results – I. SED deconvolution analysis

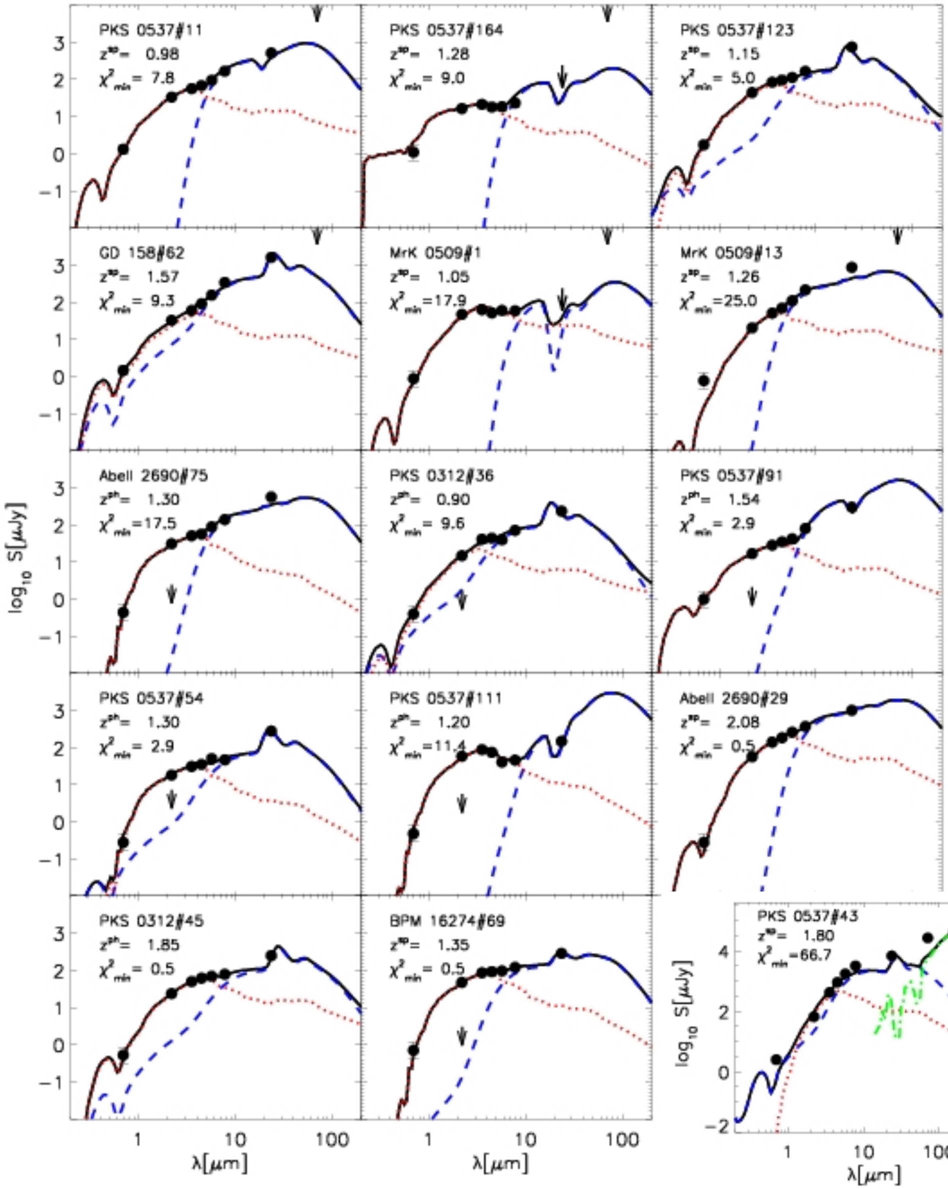

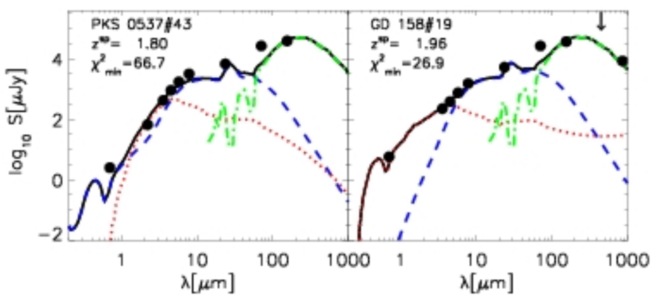

Pozzi et al., A&A 2010, in press (arXiv: 1003.5563)

Torus (AGN)

Host Galaxy

✓ Typically, good fits to the R, K_S and *Spitzer* data

✓ Host galaxy required, prominent for extreme X/O sources

✓ Nucleus starts dominating at the longest-λ IRAC bands

✓ 80% of sources have τ(9.7μm)<3

Results – II. "Corrections" to the observed L_{bol}

Mainly geometric correction factor

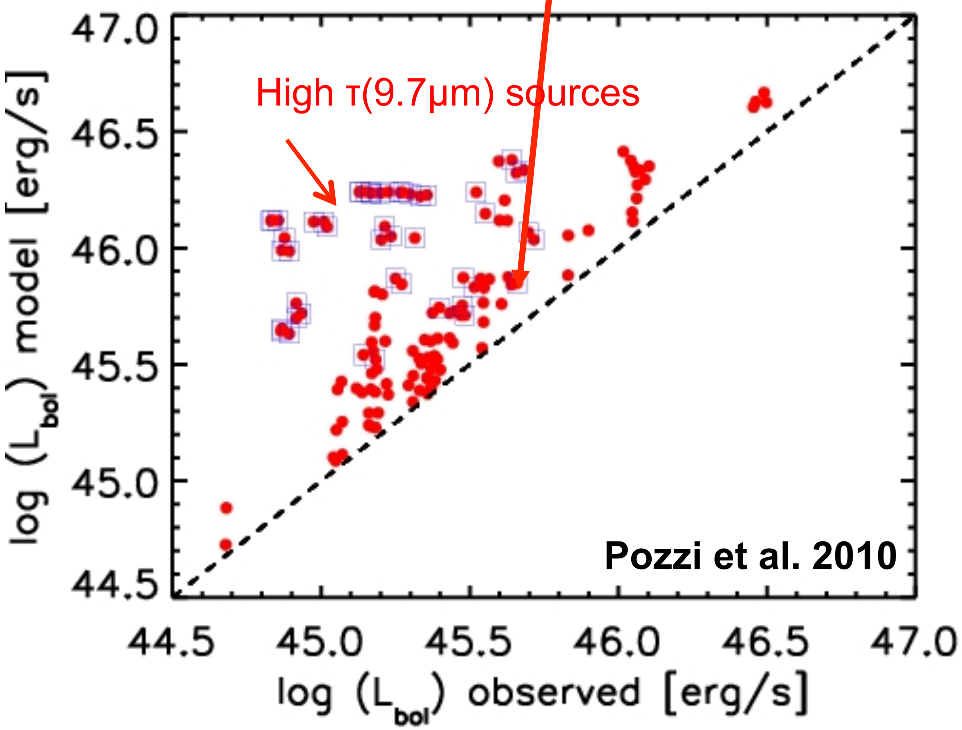

Only a fraction of the intrinsic accretion disc radiation is intercepted by the torus (function of the covering factor

$$CF = (4\pi - 2\pi\,(1+\cos\Theta))/\,4\pi$$

+

Dust self-absorption effects for large $\tau(9.7\mu m)$

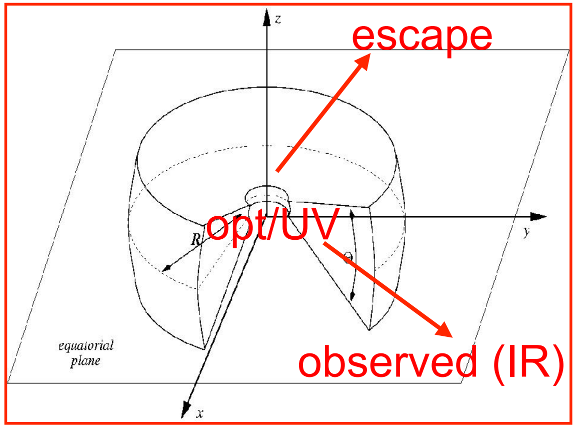

L_{bol} (model) = L (accr, from SED fitting) + L_X

L_{bol} (observed) = L_{IR} + L_X

➔ L_{bol} (model) ≈ 2 × L_{bol} (observed)

Results – III. AGN bolometric corrections

$$K_{bol,X} = \frac{L_{bol,mod}}{L_{2\text{-}10\,keV}}$$

Keep in mind: hard X-ray selected sample

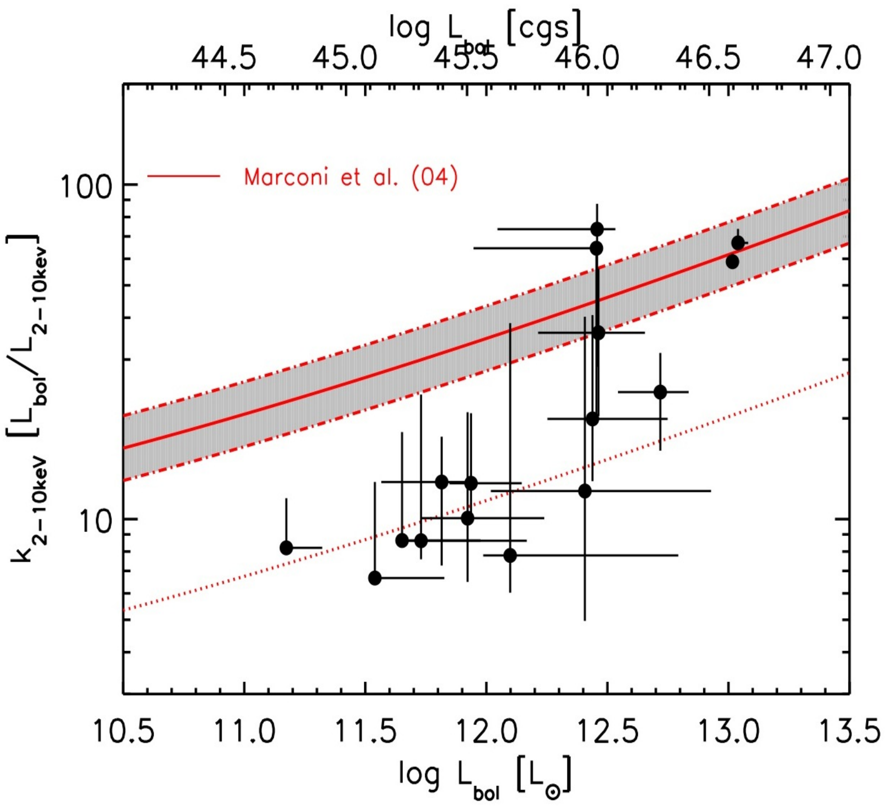

$L_{BOL} \approx 6\times10^{44}-4\times10^{46}$ erg/s

$K_{2\text{-}10\,keV} \approx 20$ (median), with large spread

Similar to large (≈540) Type 1 QSOs in XMM-COSMOS (Lusso et al. 2010)

For comparison:

- ✓ ≈30 in Type 1 QSOs from Elvis+94 but large dispersion in the broad-line QSO SEDs
- ✓ X-ray luminous ($Lx \approx 10^{43\text{-}46}$ erg/s) AGN by Kuraszkiewicz+03: k≈18
- ✓ low-luminosity ($Lx \approx 10^{42\text{-}43.6}$ erg/s) AGN by Ballo +07; k≈12

Systematically lower than predicted by Marconi et al. (2004)

Results – IIIb. Black hole masses

M_{BH} from local Marconi & Hunt (2003) relation

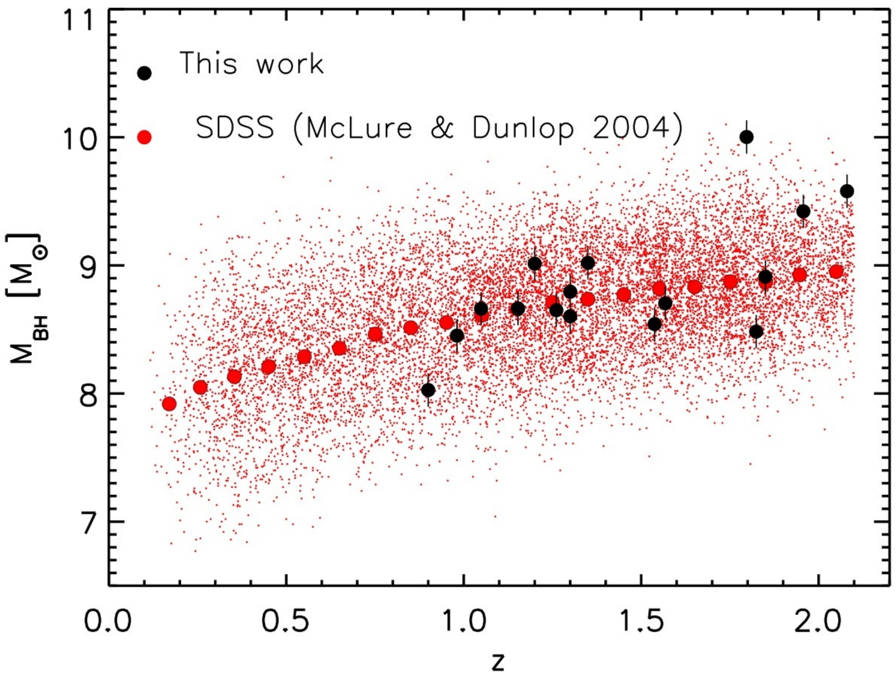

Median $M_{BH} \approx 5 \times 10^8\ M_\odot$

In relatively good agreement with the SDSS Type 1 QSO compilation from McLure & Dunlop (2004)

and the results for X-ray selected (XMM-COSMOS) Type 1 QSOs in the same redshift range (median $M_{BH} \approx 3.2 \times 10^8\ M_\odot$)

Results – IV. Eddington ratios

$$\lambda = \frac{L_{bol}}{L_{Edd}}$$

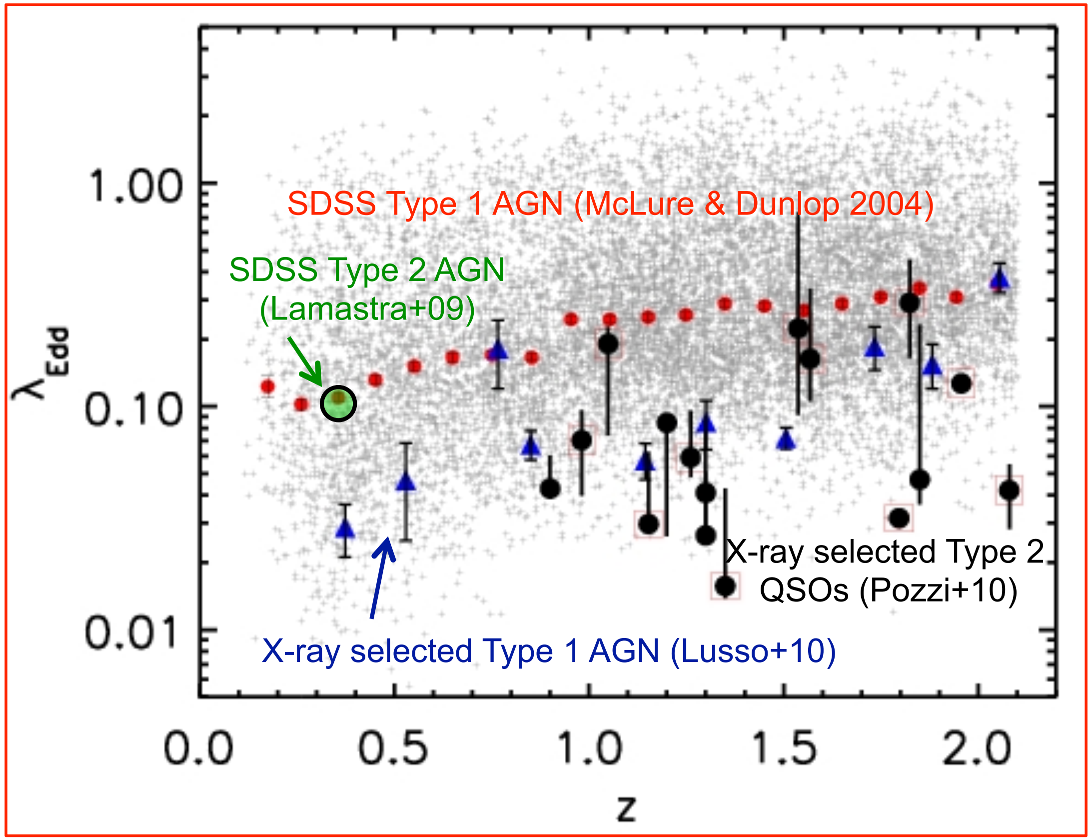

median λ≈0.08

Lower than SDSS in the same redshift interval

Consistent with XMM-COSMOS Type 1 AGN (Lusso et al. 2010)

Effect of X-ray selection?

Results – V. Eddington ratios vs. bolometric corrections

Comparison with Vasudevan & Fabian results

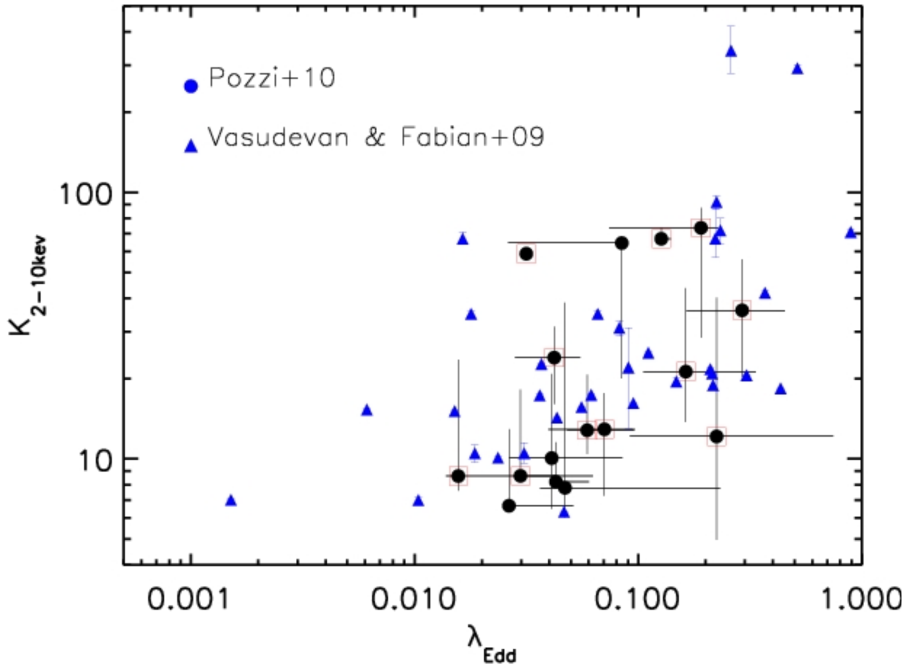

Agreement with XMM-COSMOS results for Type 1 AGN (Lusso et al. 2010)

k_{bol}≈22 for λ≤0.1, k_{bol}≈27 for 0.1<λ≤0.2, and *k_{bol}≈53 for λ>0.2*

Recent indications for a trend of increasing K_{bol} at increasing Eddington ratios using a sample of AGN with simultaneous UV/X-ray observations

SED=function(λ_{Edd}), different fraction of ionizing UV photons

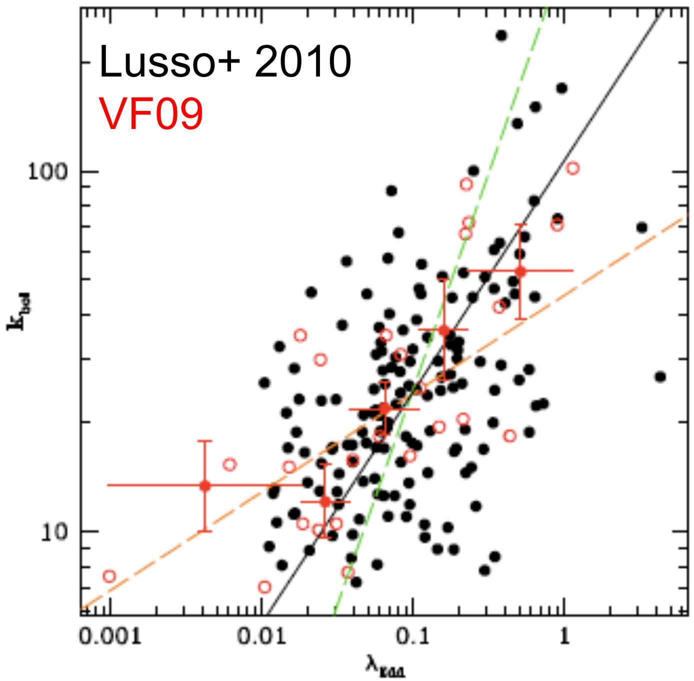

"clumpy" vs. "smooth" torus models applied to IRAS 09104+4109

See also A. Feltre's talk

Obscured, luminous QSO at z=0.442
Overall, good modeling with both smooth and clumpy solutions but need for an extra hot dust component (T≈1400 K) in clumpy models (Mor et al. 2009; Nikutta et al. 2009; Deo et al. 2011; Mor & Trakhtenbrot 2011)

Smooth torus

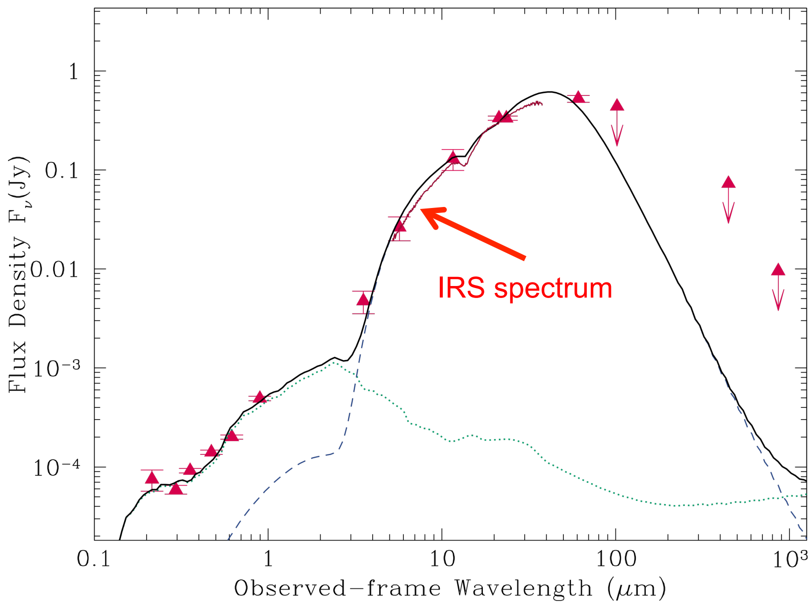

Clumpy torus

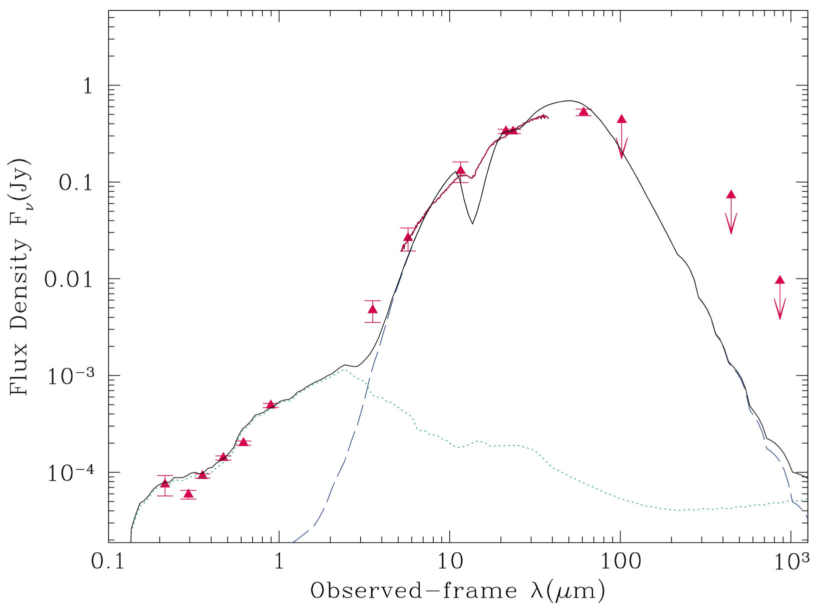

A case of coeval AGN and star-forming activity among obscured QSOs at $z \approx 2$

Similar cases reported in Page et al. (2001, 2004, 2011), Stevens et al. (2004), Mainieri et al. (2005), Polletta et al. (2008), Aravena et al. (2008), Brusa et al. (2010), Feruglio et al. 2011, Gilli et al. (2011)

The BH/galaxy “evolutionary model”

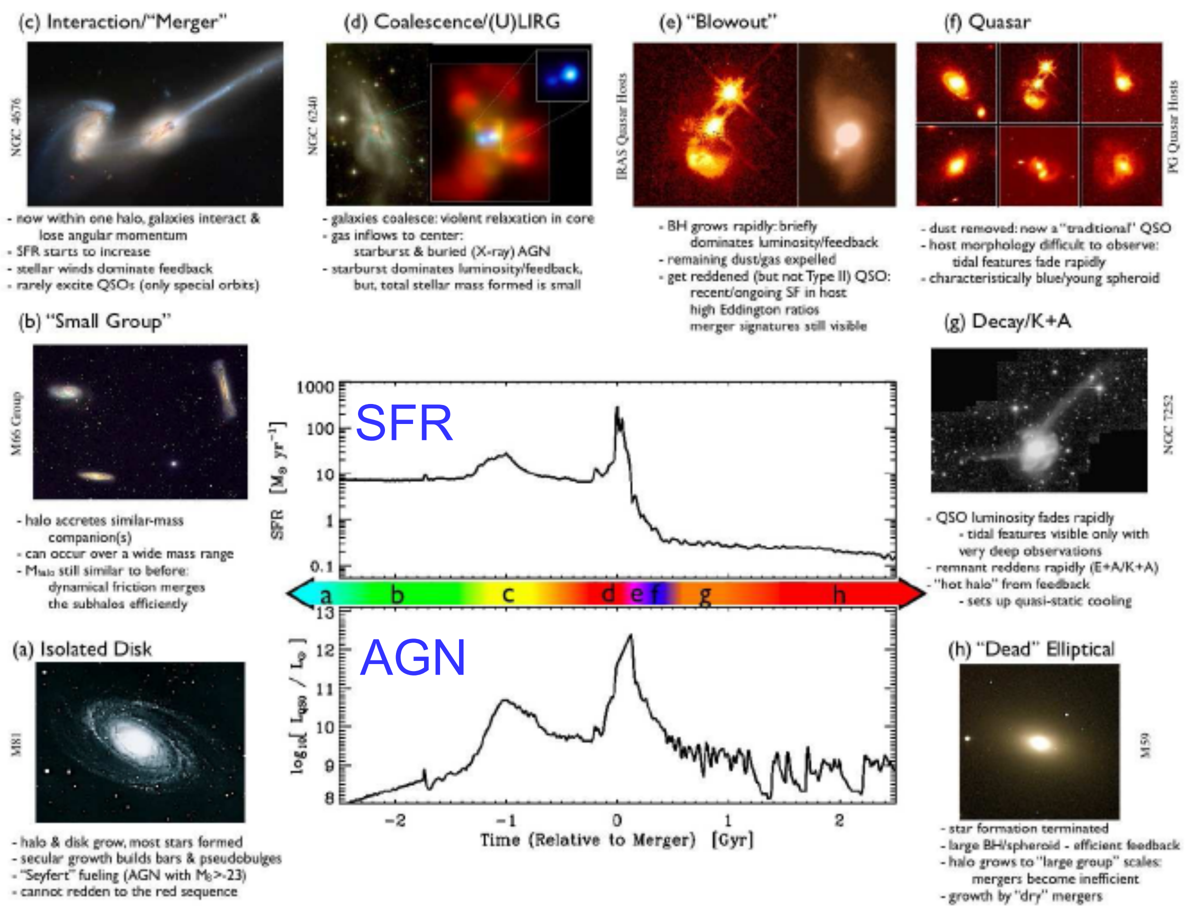

Hopkins+08; see also Di Matteo +05, Menci+08, Sanders+88, Fabian 99, […]

Winds likely play a significant role in quenching star formation (outflows and ionized absorbers; e.g., Alexander+10, Page+11)

mergers

SF/obscured accretion

“clean” accretion (QSO)

transition (green valley) object

passive red galaxy

Can explain several observables:

- local BH/galaxy scaling relations
- local BH mass function
- QSO luminosity function
- QSO clustering
- host galaxy colors

Scientific Background

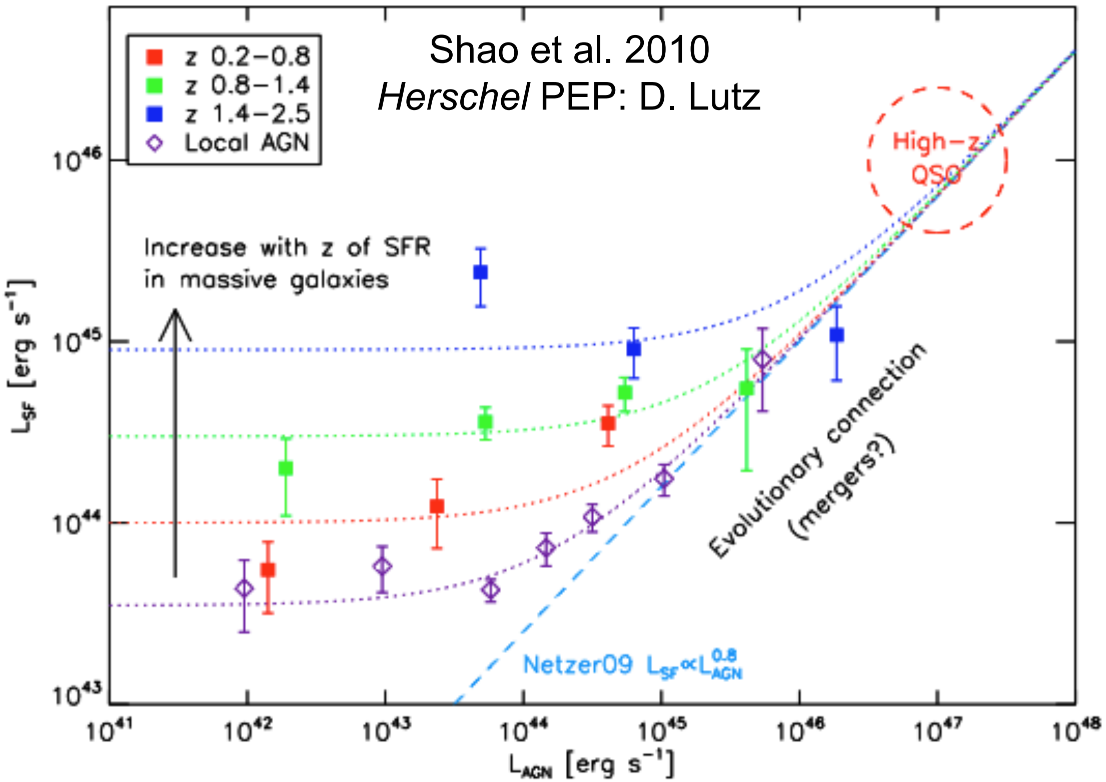

Two paths of AGN/galaxy co-evolution

• At high AGN luminosity, galaxy merging is the driver of accretion and star formation ➔ rapid bursts of activity

• At lower AGN luminosity, SF has little dependence on AGN luminosity ➔ secular, non-merger driven star formation

(e.g. Georgakakis+09, Lutz+10, Cisternas+11, Schawinski+11, Elbaz +11)

Already discussed by D. Lutz yesterday

Optical and X-ray properties

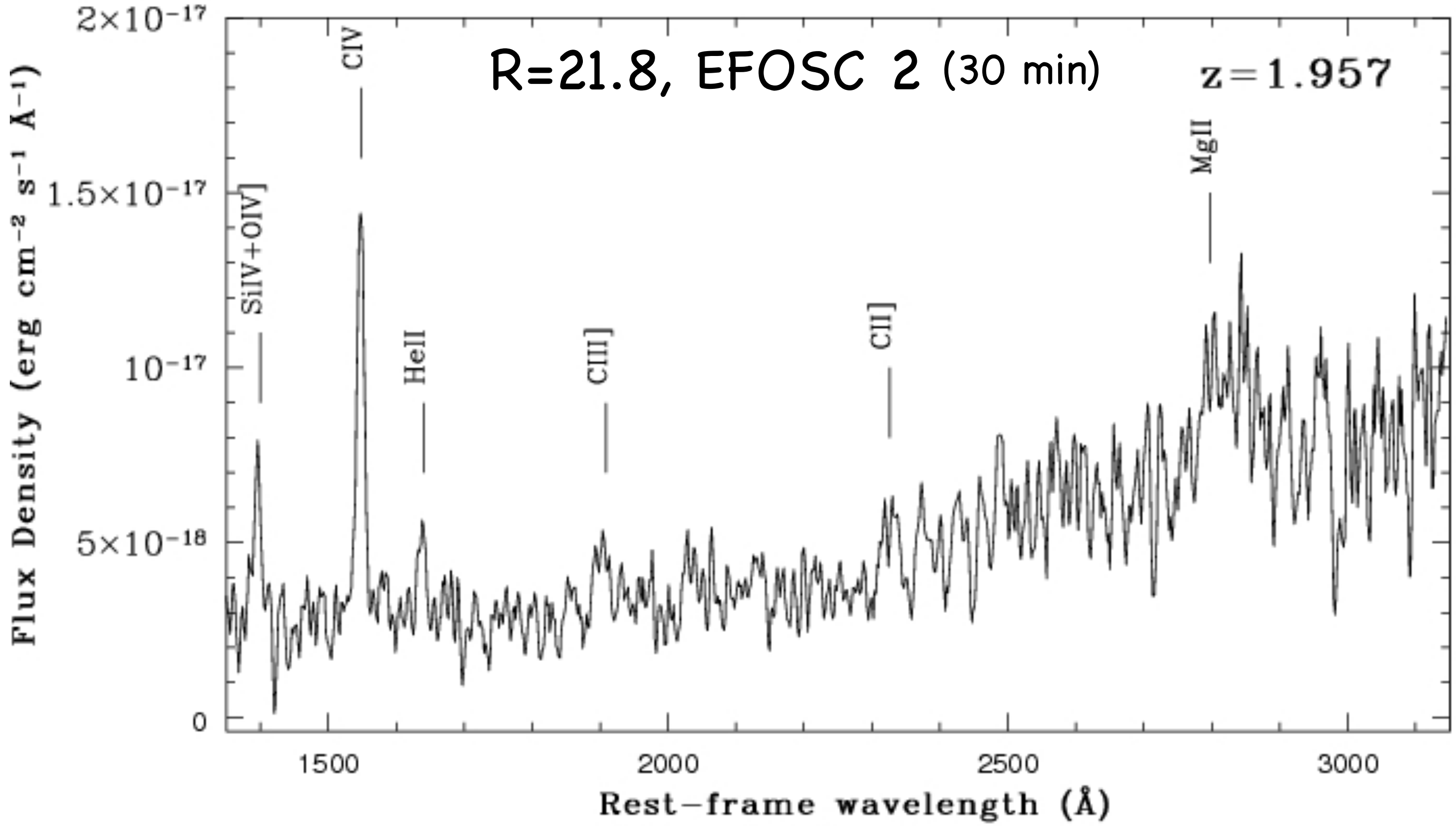

Optical: narrow (FWHM<1500 km/s) emission lines
red continuum
hints of a broad MgII but noisy spectrum
line EWs and ratios different from SDSS Type 1 QSOs

X-ray: $L_{2\text{-}10\ keV} \approx 6\times10^{44}$ erg/s
$N_H \approx 7\times10^{22}$ cm^{-2}

The *Spitzer* view of H2XMMJ003357.2−120038 at z=1.957

3.6 4.5 5.8 8.0 micron

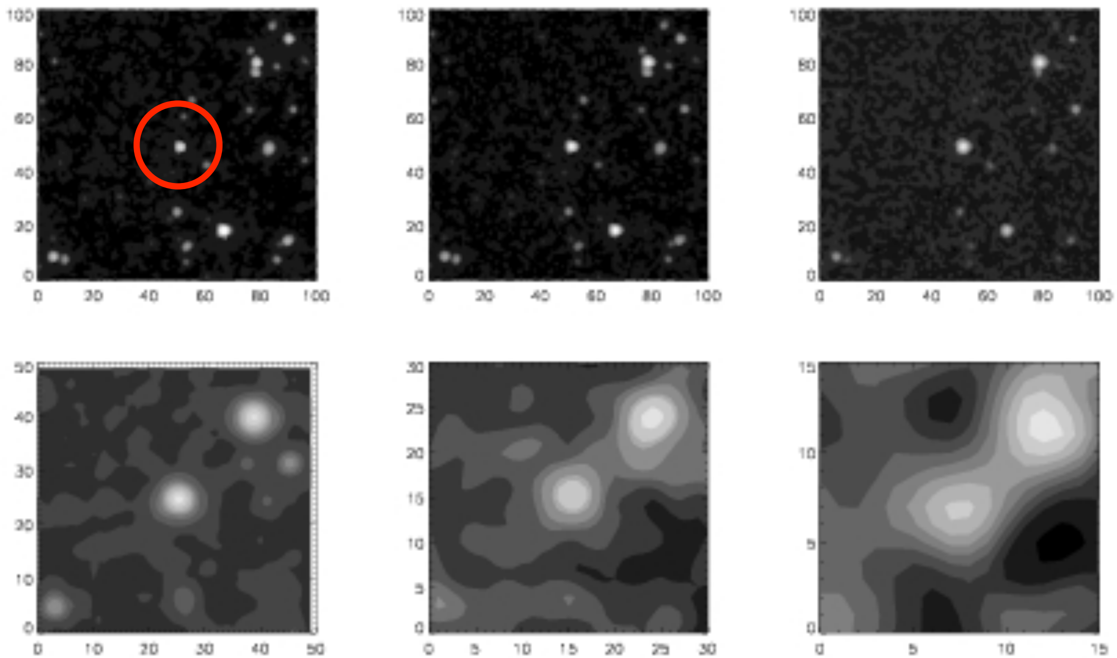

+SCUBA at 850 μm

24 70 160 micron

Broad-band SED fitting

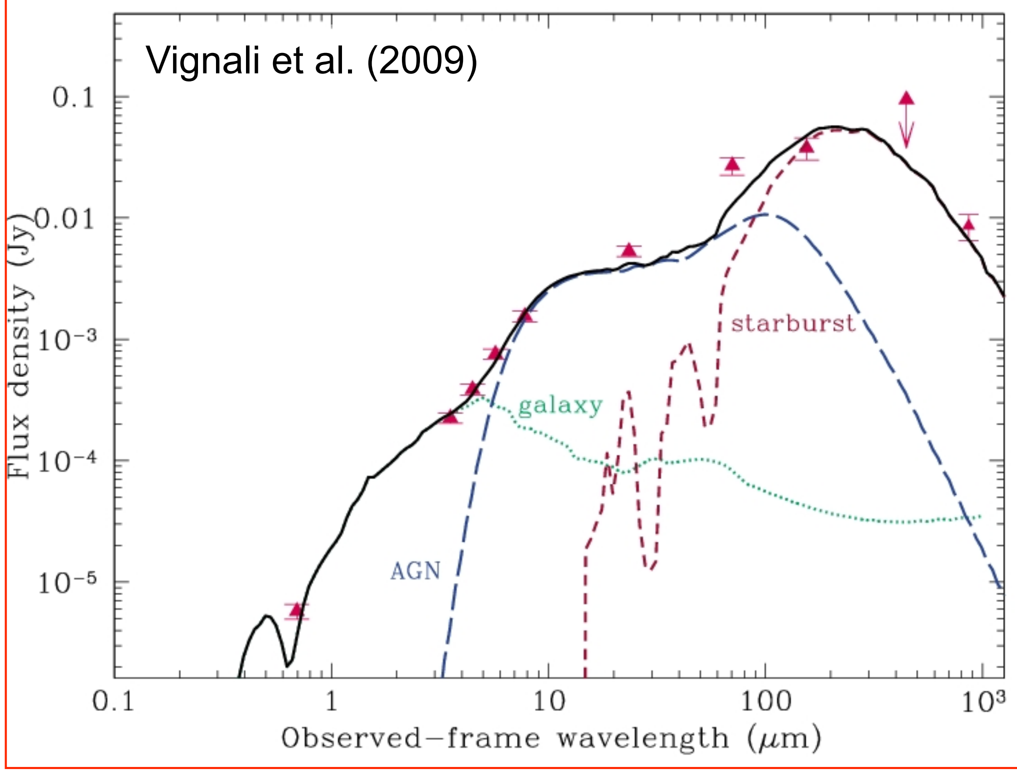

- τ (9.7) ≈1.0
- covering angle≈140 deg
- SFR≈1500 $M_{\odot}$/yr
- ≈54% is the AGN contribution to the 1-1000 μm

Using MH03: M_{BH}≈1.9x10^9 $M_{\odot}$

L_{bol}=4.3x10^{46} erg/s

⇒ λ=Edd. ratio≈0.19

A similar case in the early Universe:
a ULIRG/Compton-thick QSO at z=4.76 in the CDF-S

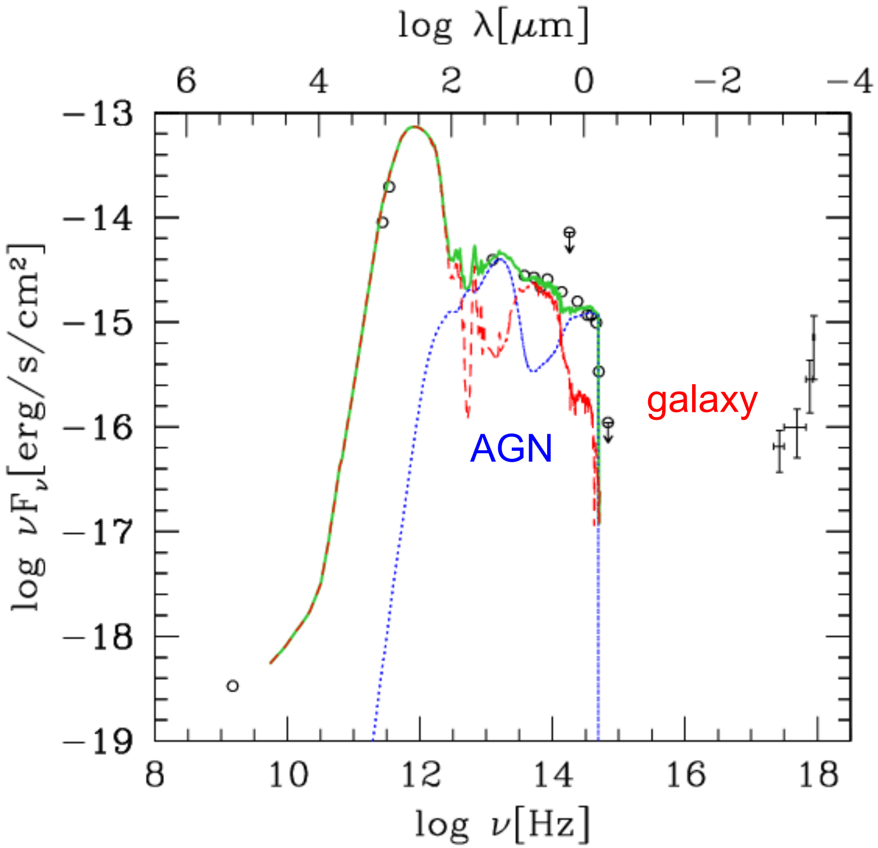

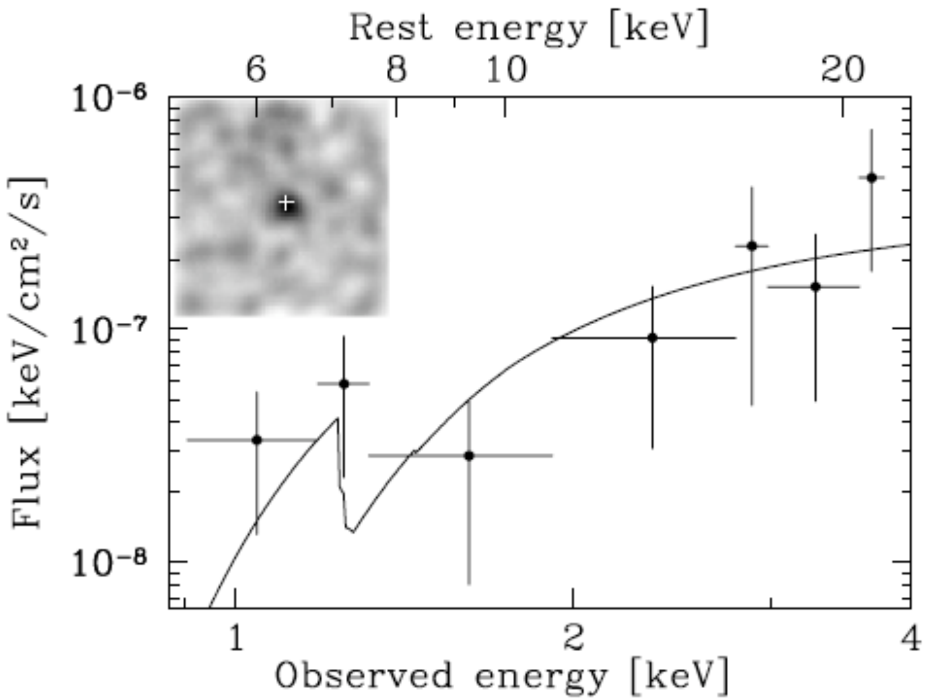

Gilli+11

SFR≈1000 $M_{\odot}$/yr (Coppin+09)
M_{H2}>10^{10} $M_{\odot}$, M_{dust}≈5×10^{8} $M_{\odot}$
L_{SB}≈2×10^{46} erg/s
L_{AGN}≈7×10^{45} erg/s
L_{AGN}~L_{SB}/3 ➔ AGN energetically relevant

Fs=4×10^{-17}, Fh=7×10^{-16} erg/cm^2/s
Lx≈2.5 ×10^{44} erg/s, N_H≈1.4×10^{24} cm^{-2}
Only possible to get this with 4Ms *Chandra*

Good science case for ALMA!

Examples from literature – I

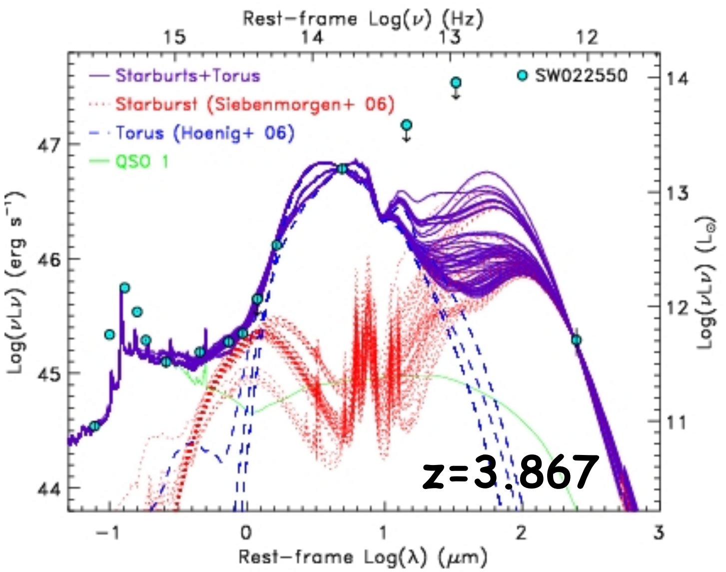

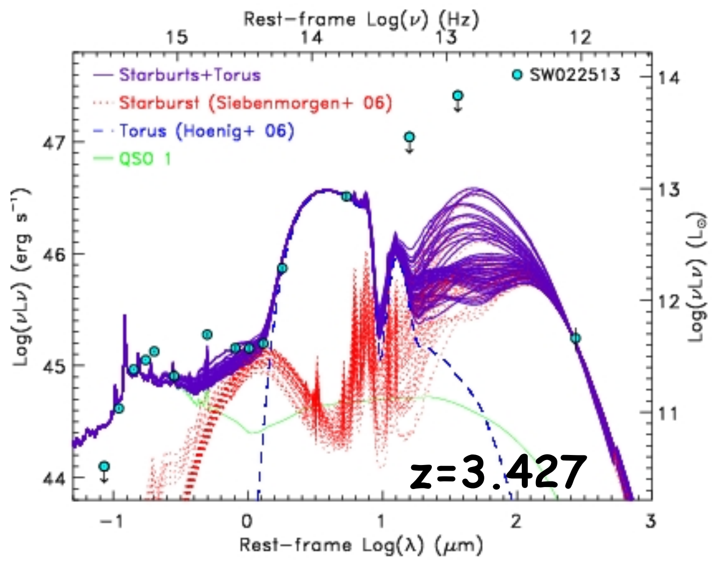

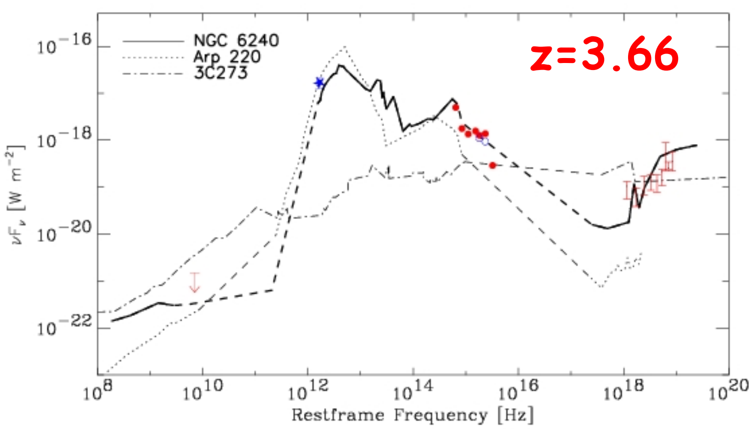

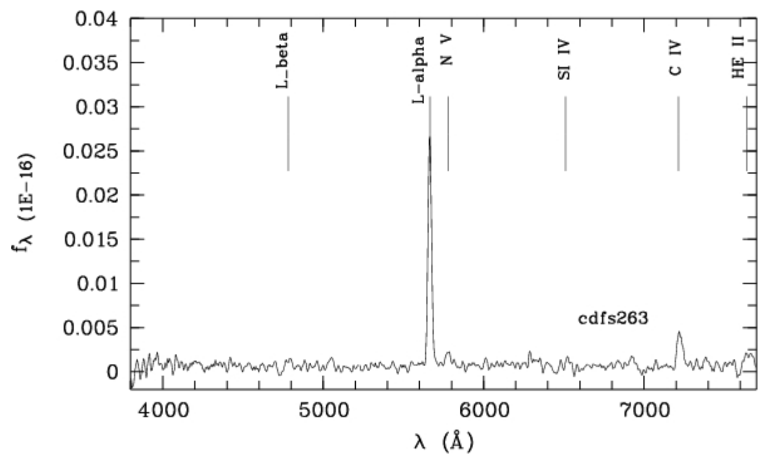

Examples from literature – II

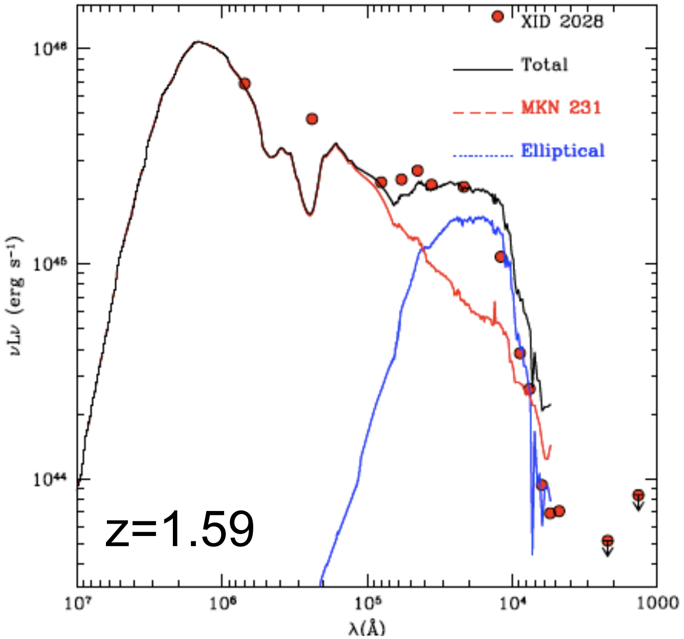

From XMM-COSMOS (Brusa+10)

z=1.59, R-K=6.5, Log X/O=1.8, $L_{2\text{-}10\,keV}=10^{45}$ erg/s, Log N_H=22

SFR≈1000 M/yr

Obscured QSO + intense SF

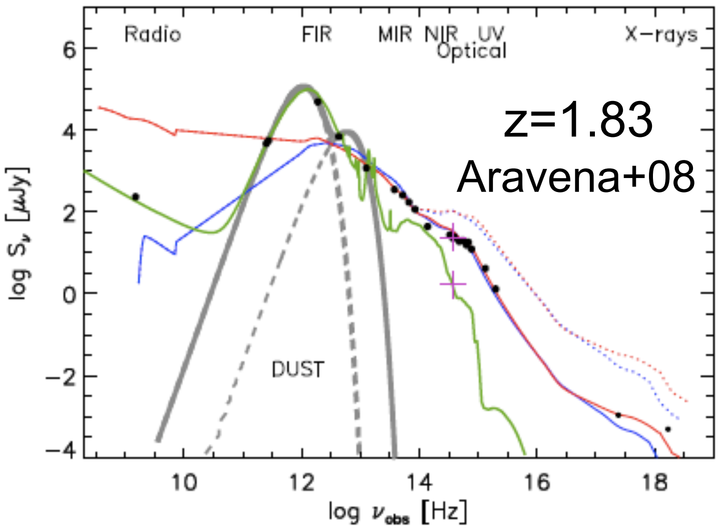

From COSMOS (Aravena+08)

z=1.83, broad MgII, molecular gas content + dust properties typical of SMGs + tidal tails suggestive of merging

SFR≈1700 $M_{\odot}$/yr

Examples from literature − III
Obscured quasars at high redshifts

Page+01, 04; Stevens+04, 06

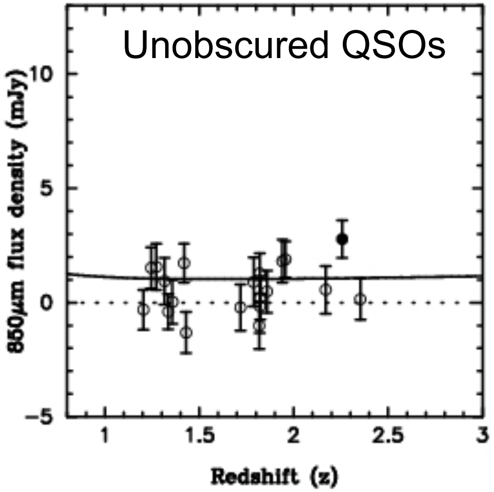

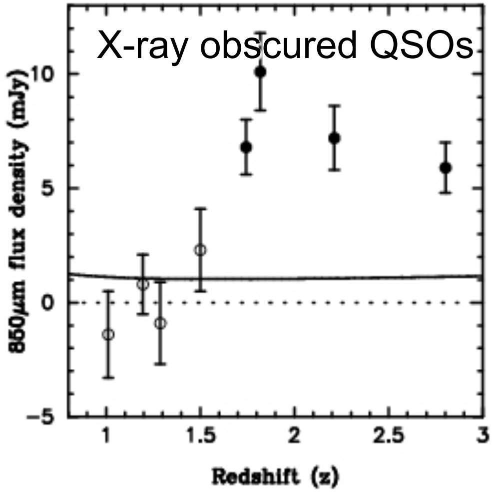

Broad-line quasars at z=1.5-3
obscured in X-rays
SFR>1000 $M_{\odot}$/yr
sub-mm-detected

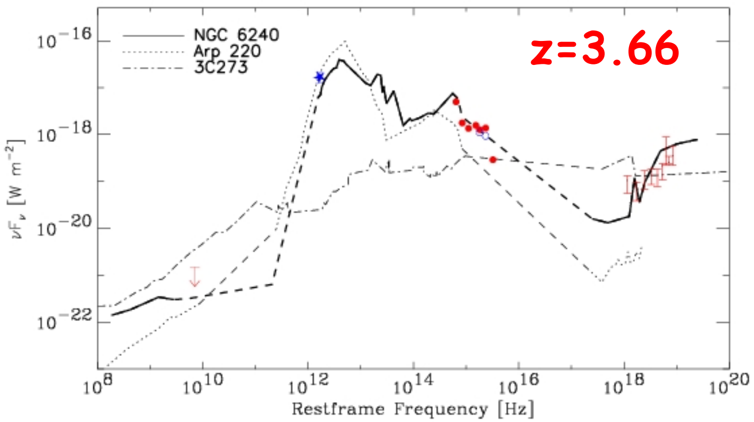

Mainieri+ 05

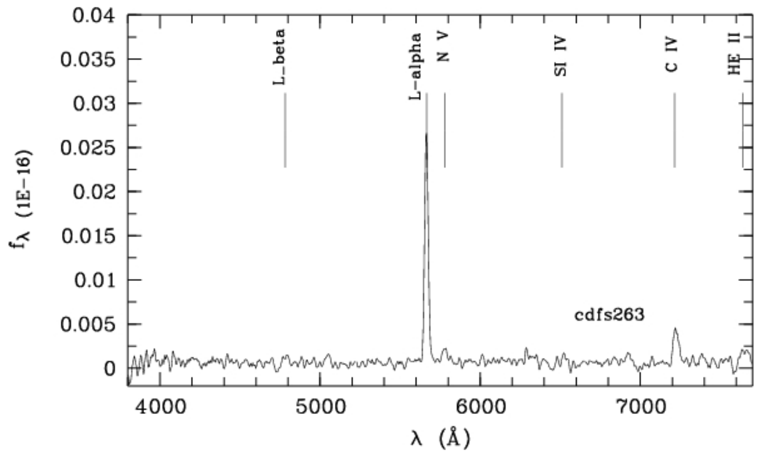

SFR=550-680 $M_{\odot}$/yr, sub-mm-detected

Examples from literature − IV

Compton-thick AGN in BzK galaxies at z=2.5-3 in the CDF-S

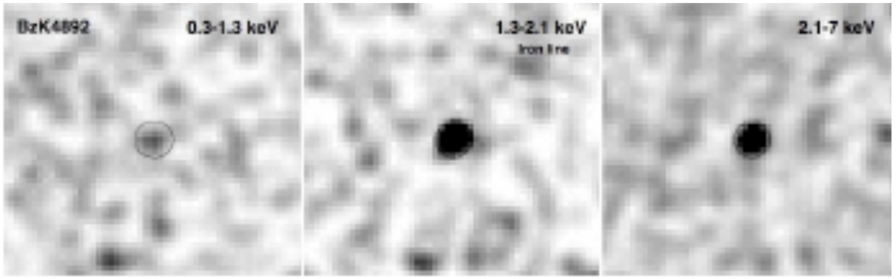

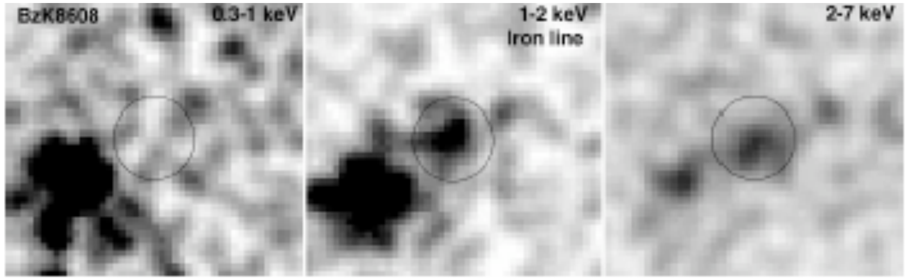

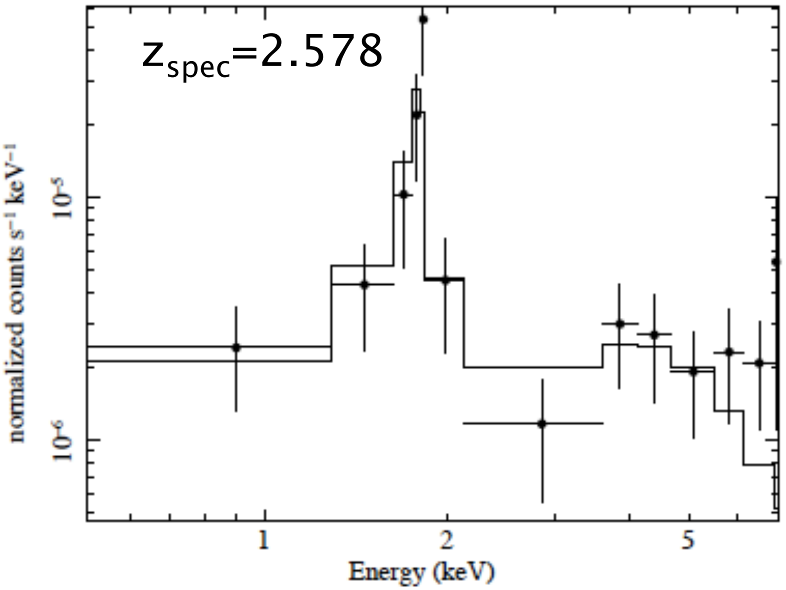

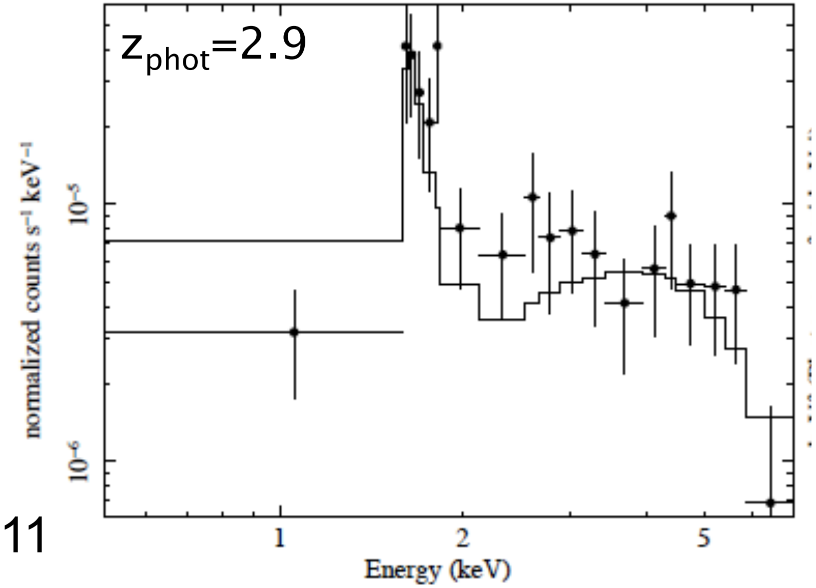

Feruglio+11

EW (Fe Kα)≈2.3 keV, NH>>10^{24} cm^{-2}

L(2-10 keV)≈$10^{44.5}$ erg/s, most likely 10^{45} erg/s (derived from Fe Kα, mid-IR , and optical lines)

EW(Fe Kα)≈1.2 keV, NH>a few 10^{24} cm^{-2}

L(2-10 keV)≈10^{44} erg/s

SFR≈300−700 $M_\odot$/yr

II sample: ULIRGs at $z \approx 2$. Constraints to the AGN emission via SED fitting of mid- and far-IR data + IRS spectroscopy

Mid-IR selected ULIRGs in the GOODS-South Field

Starting sample: 24 ULIRGs with S(24 μm)≈150−600 μJy at z≈1.7−2.2
with ultra-deep IRS spectroscopy (Fadda et al. 2010)
Major contributors to z=2 IR background

GOAL: use optical + *Spitzer* data points + IRS spectroscopy + far-IR Herschel data (PEP; P.I. D. Lutz) to reproduce the SED and estimate the role played by AGN (torus) emission
Compare with X-ray emission (4Ms source catalog; Xue+2011)

Relevant AGN emission

IRS spectra: courtesy of D. Fadda

Pozzi et al, work in progress

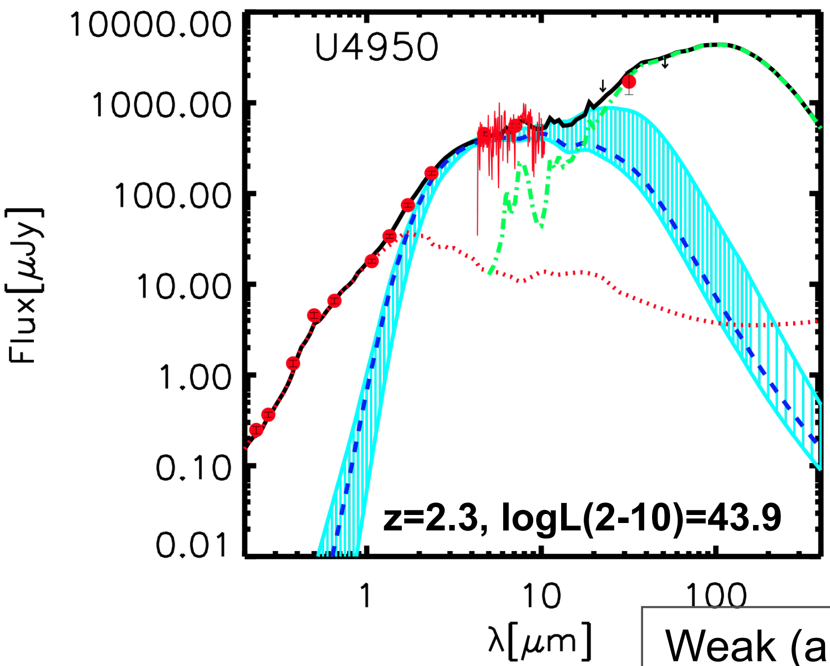

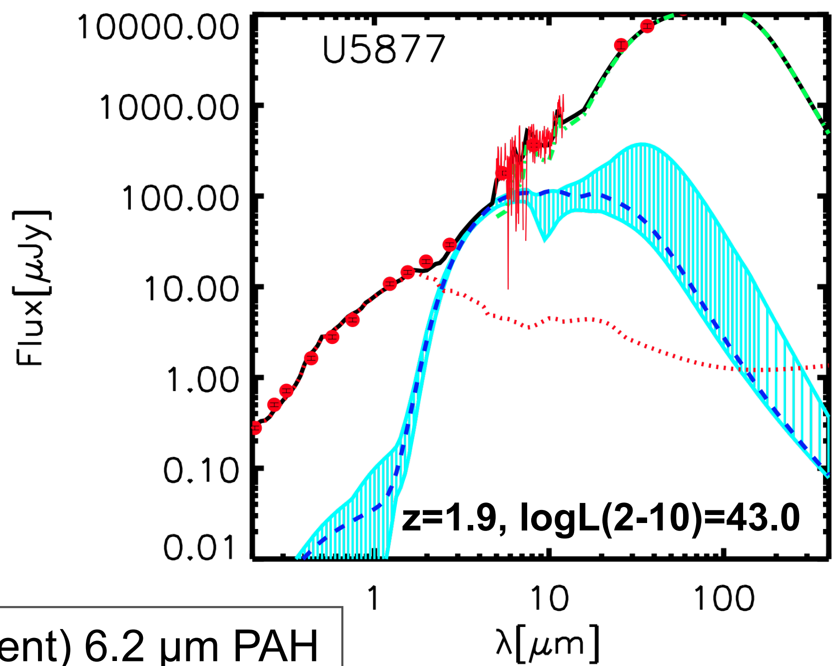

Weak (absent) 6.2 μm PAH

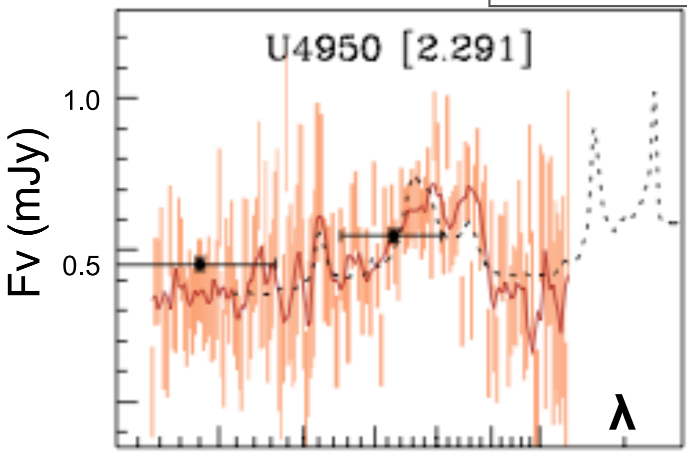

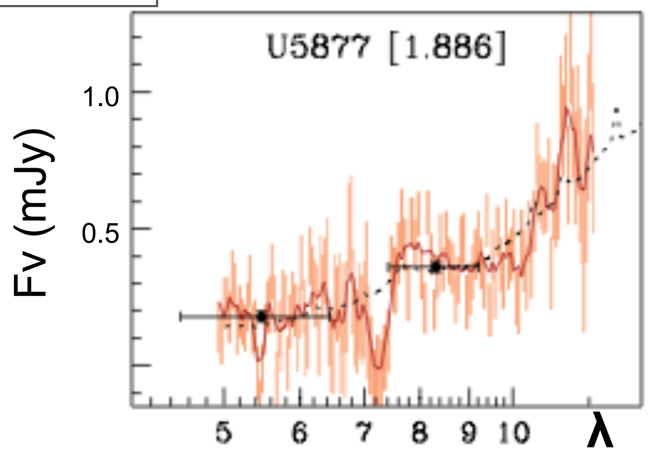

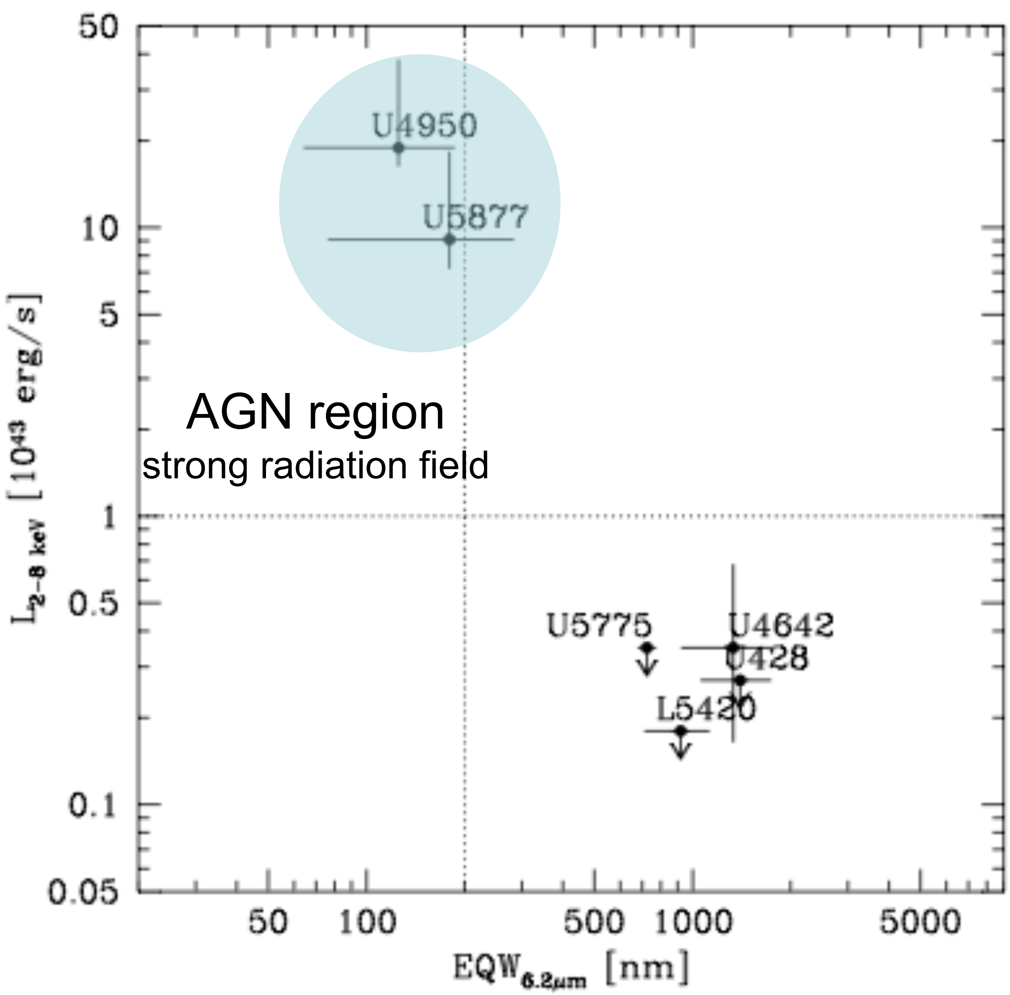

AGN region
strong radiation field
U4950
U5877
U5775
U4642
U428
L5420
50
10
5
1
0.5
0.1
0.05
50
100
500
1000
5000
L2-8 keV [10^43 erg/s]
EQW6.2μm [nm]

Fadda+10

No AGN required

IRS spectra: courtesy of D. Fadda

Work in progress

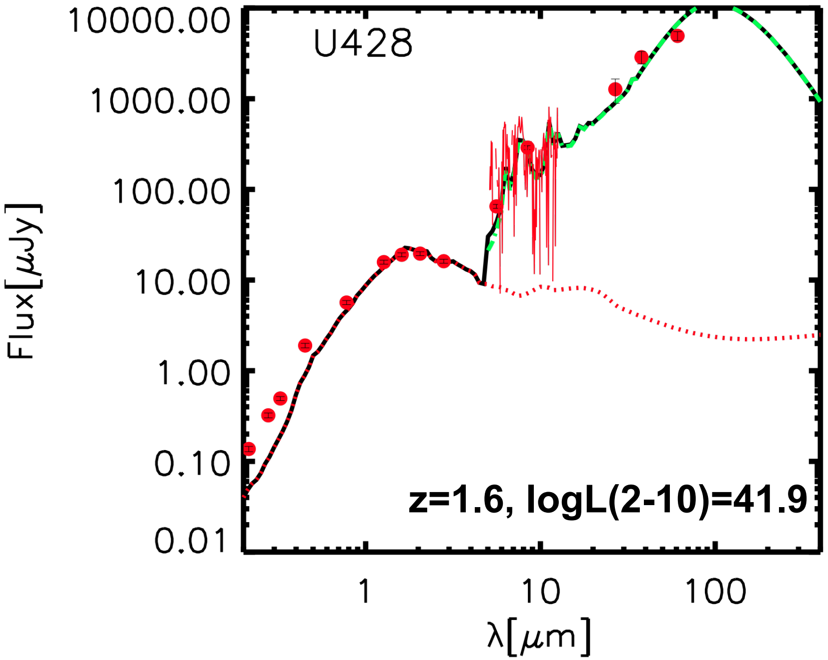

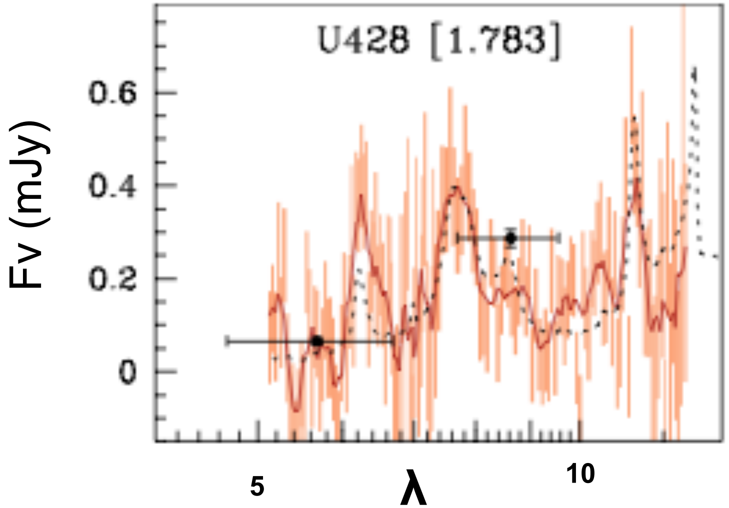

Detection of the 6.2 μm PAH

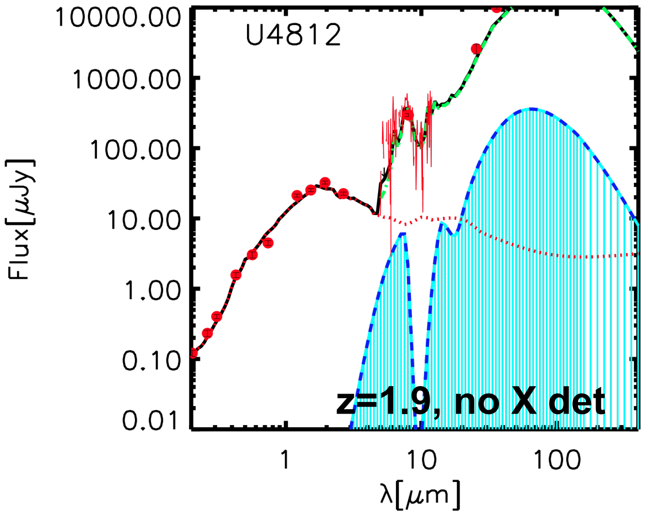

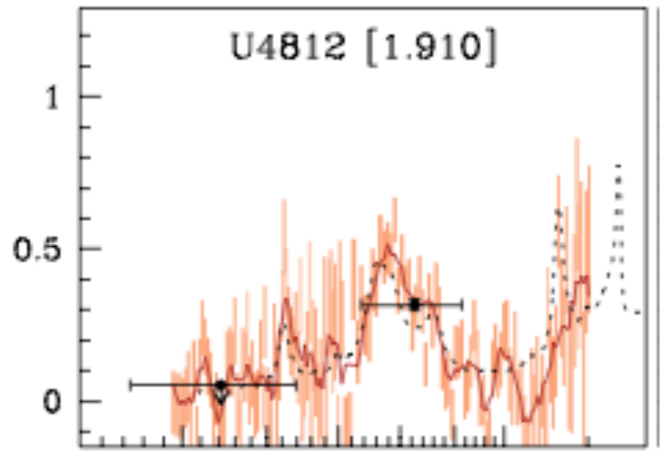

“Intermediate” cases

IRS spectra: courtesy of D. Fadda

Work in progress

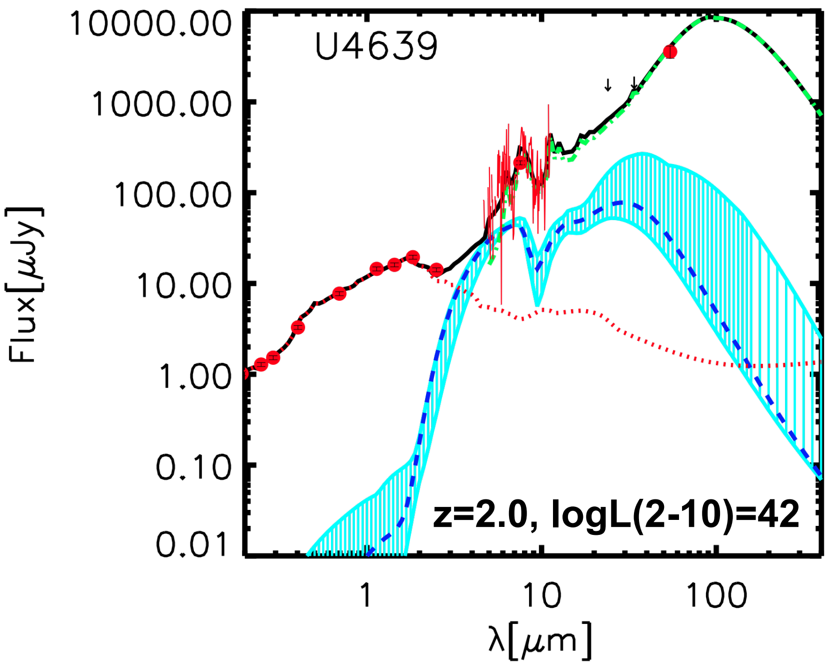

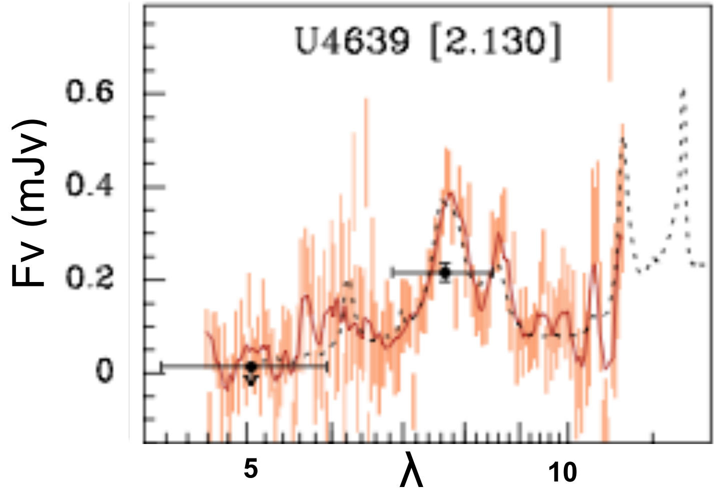

Detection of the 6.2 μm PAH

Sample properties: AGN contribution from SED fitting

Next: average properties for the
individually undetected sources (X-ray stacking)

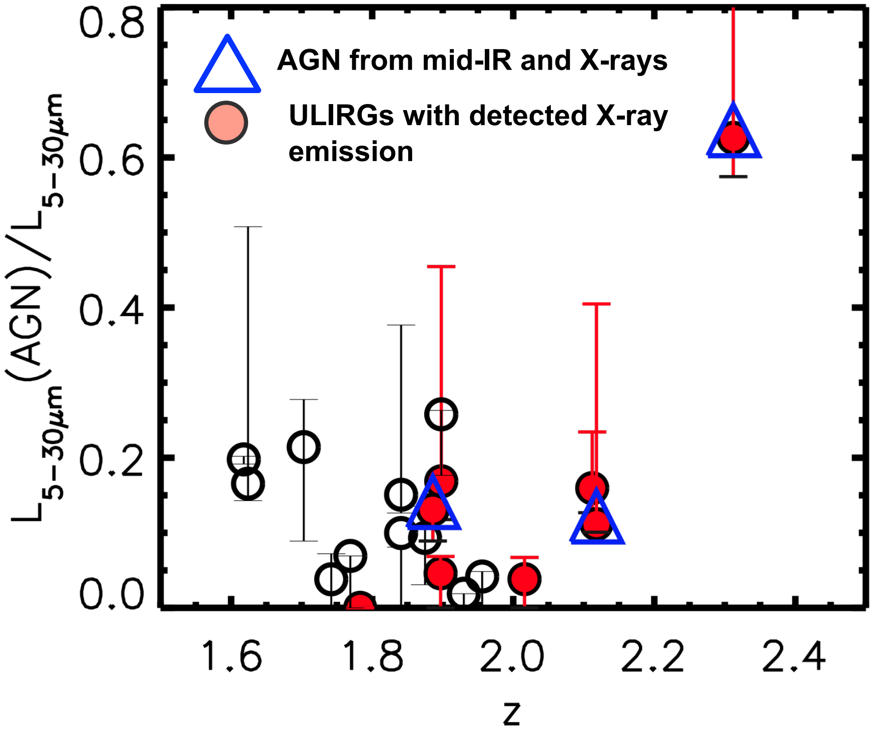

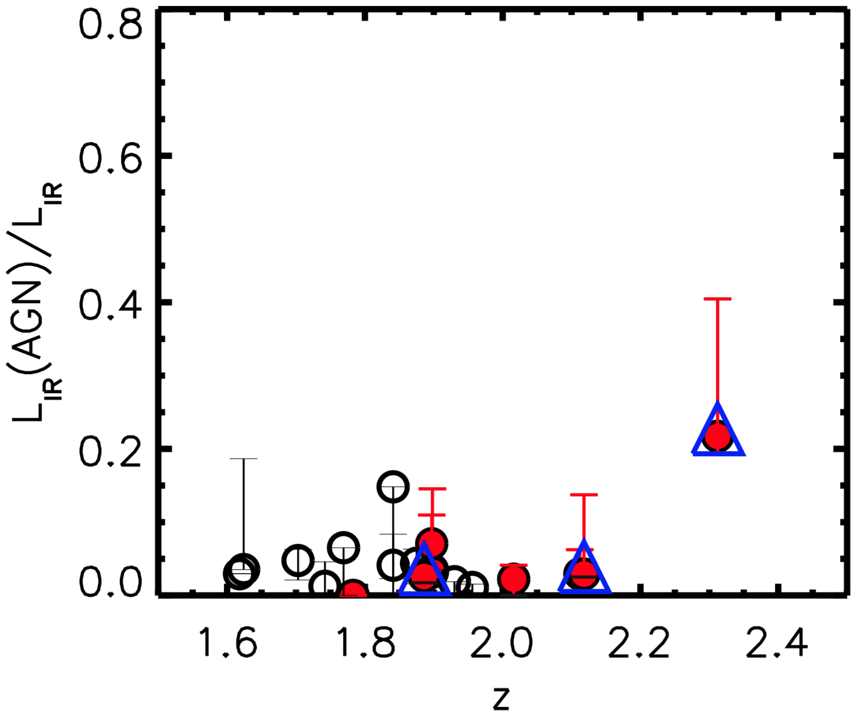

❑ ≈12% AGN (torus) contribution to the mid-IR
❑ ≈20% excluding sources whose SED fitting does not required an AGN component

❑ ≈3% AGN contribution to the far-IR
❑ ≈5% excluding sources whose SED fitting does not required an AGN component

Further clues on the mid-IR emission from the AGN

L(2-10 keV) predicted using the **12.3 μm (computed from the SED fitting)** vs. hard X-ray luminosity correlation from Gandhi et al. (2009) − sample of Seyfert galaxies with high-resolution (diffraction-limited) mid-IR imaging

Possible cause of discrepancy: X-ray obscuration − currently not takein into account − or problems with SED fitting

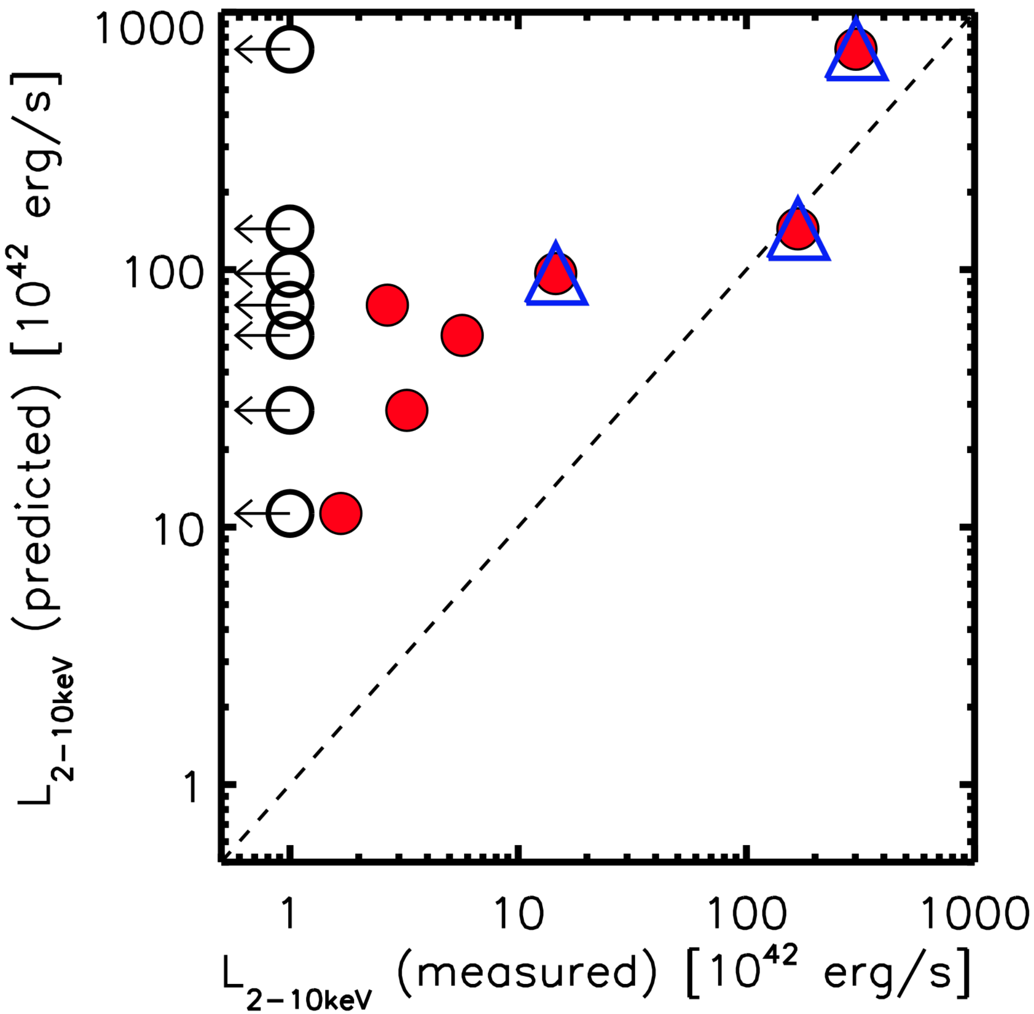

The importance of mid-IR/far-IR spectroscopy: The case of *SPICA*-Safari (JAXA/ESA)

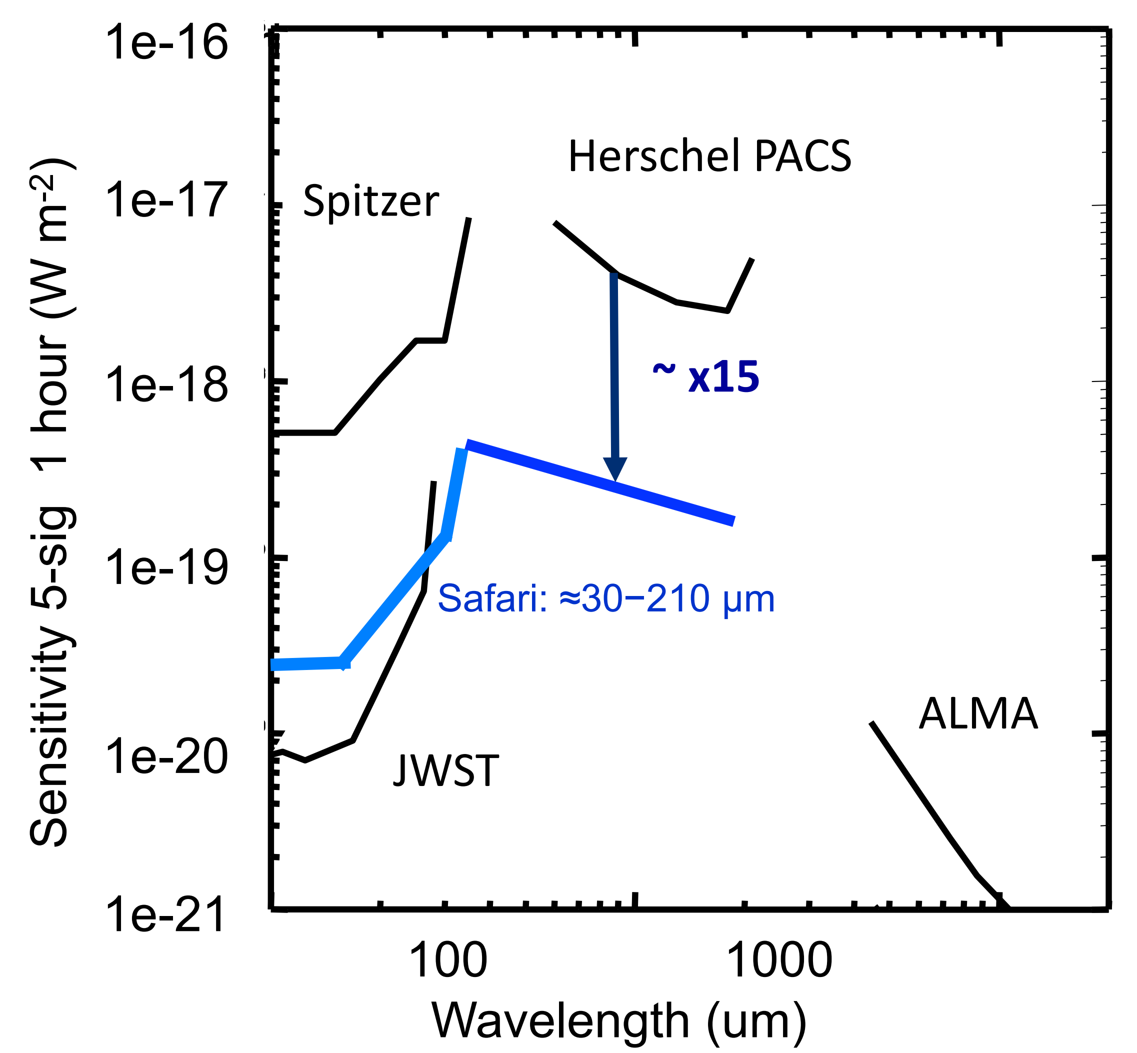

FTS can cover multiple lines over a relatively large field-of-view

The multiplex advantage

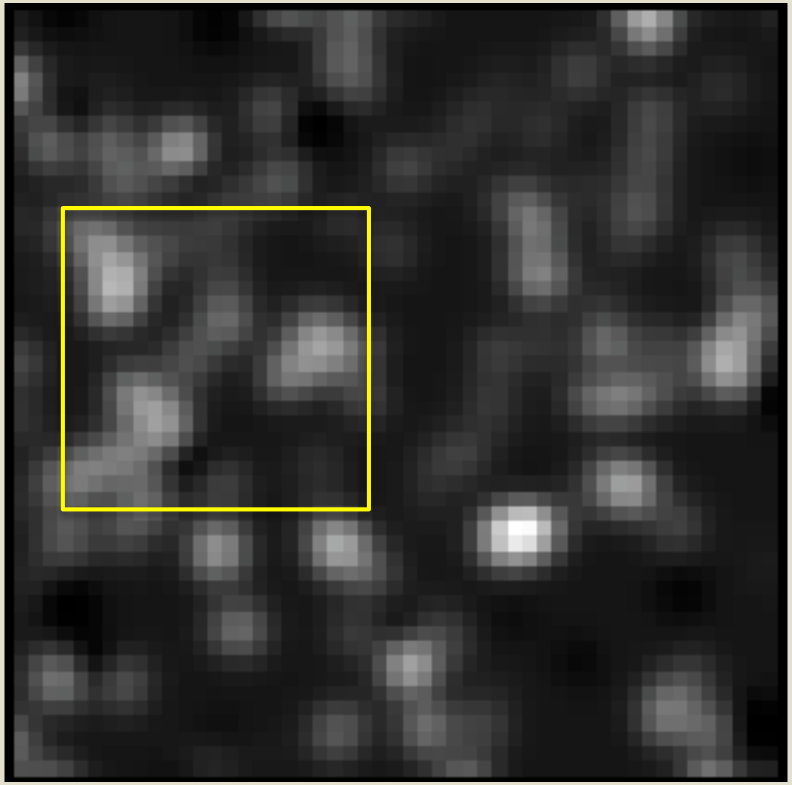

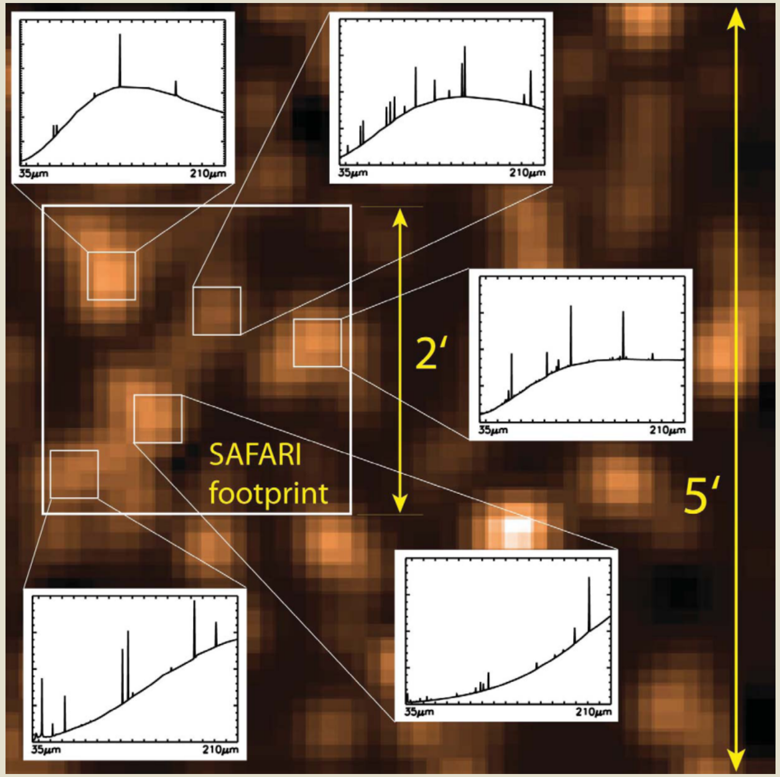

SPICA FIR FTS will take spectra of 7-10 sources/field

Images from Rosenboom, Oliver, Smith, Raab

Summary

- X-ray obscured luminous quasars at z≈1-2 are well reproduced by smooth torus models. Eddington ratios and bolometric corrections are consistent with other X-ray selected AGN samples

- Coeval obscured accretion and star formation is expected in terms of AGN "evolutionary sequence" but this self-consistent picture must be sharpened on many respects. Test science case for ALMA imaging and spectroscopic capabilities

- Mid-IR selected ULIRGs at z≈2 have on average little contribution from AGN. SED fitting + ultra-deep X-ray observations are needed to place constraints

- Mid-IR and far-IR spectroscopy (*SPICA*-Safari) can open new windows in molecular physics of AGN and galaxies at high redshift

The End